Optimal Patching in Clustered Malware Epidemics

Soheil Eshghi, *Member, IEEE*, M. H. R. Khouzani, Saswati Sarkar, *Member, IEEE*, and Santosh S. Venkatesh, *Senior Member, IEEE*

***Abstract*—Studies on the propagation of malware in mobile networks have revealed that the spread of malware can be highly inhomogeneous. Platform diversity, contact list utilization by the malware, clustering in the network structure, etc., can also lead to differing spreading rates. In this paper, a general formal framework is proposed for leveraging such heterogeneity to derive optimal patching policies that attain the minimum aggregate cost due to the spread of malware and the surcharge of patching. Using Pontryagin's Maximum Principle for a stratified epidemic model, it is analytically proven that in the mean-field deterministic regime, optimal patch disseminations are simple single-threshold policies. These policies are amenable to implementation and can serve as benchmarks for policies that have less knowledge of the network. Through numerical simulations, the behavior of optimal patching policies is investigated in sample topologies, and their advantages are demonstrated.**

***Index Terms*—Belief propagation, immunization and healing, security, technology adoption, wireless networks.**

I. Introduction

WORMS (self-propagating malicious codes) are a decades-old threat in the realm of the Internet. Worms undermine the network in various ways: They can eavesdrop on and analyze traversing data, access privileged information, hijack sessions, disrupt network functions such as routing, etc. Although the Internet is the traditional arena for trojans, spyware, and viruses, the current boom in mobile devices, combined with their spectacular software and hardware capabilities, has created a tremendous opportunity for future malware. Mobile devices communicate with each other and with computers through myriad means—Bluetooth or Infrared when they are in close proximity, multimedia messages (MMS), mobile Internet, and peer-to-peer networks. Current smartphones are equipped with operating systems, CPUs, and memory powerful enough to execute complex codes. Wireless malware such as *cabir*, *skulls*, *mosquito*, and *commwarrior* have already sounded the alarm [1]. It has been theoretically predicted [2] that it is only a matter of time before major malware outbreaks are witnessed in the wireless domain.

Malware spreads when an infective node *contacts*, i.e., communicates with, a susceptible node, i.e., a node without a copy of the malware and vulnerable to it. This spread can be countered through patching [3]: The vulnerability utilized by the worm can be fixed by installing security patches that immunize the susceptible and potentially remove the malware from the infected, hence simultaneously healing and immunizing infective nodes. However, the distribution of these patches burdens the limited resources of the network and can wreak havoc on the system if not carefully controlled. In wired networks, the spread of *Welchia*, a counter-worm to thwart *Blaster*, rapidly destabilized important sections of the Internet [4]. Resource constraints are even more pronounced in wireless networks, where bandwidth is more sensitive to overload, and nodes have limited energy reserves.

1) Literature Review: Epidemic models, and especially SIR epidemic models, have been used extensively to model the spread of malware and the propagation of information in computer networks, beginning from Murray [5] and Kephart and White [6]. Recent work [7]–[9] has focused on how these epidemics can be controlled. However, the work on the propagation of information (such as [7] and [9]) has focused on two-hop routing with no adversaries, which does not apply to malware defense and a host of other applications such as technology adoption. On the other hand, works on malware defense, such as [8], have modeled healing and immunization as contact-independent exogenous processes that are uniform among all nodes, which are very limiting assumptions. Recognizing the constraints of the defender, works such as [10] and [11] have included the cost of patching in the aggregate damage of the malware and have characterized the optimal dynamic patching policies that attain desired tradeoffs between the patching efficacy and the extra taxation of network resources. Similarly, Li *et al.* [12] and Altman *et al.* [13] have characterized optimal dynamic transmission control policies for two-hop and multihop messages. These results, however, critically rely on the *homogeneous* mixing assumption: that all pairs of nodes have identical expected intercontact times. Thus, there will only be one optimal control for the system. While this assumption may serve as an approximation in cases where detailed information about the network is unavailable, studies [2], [14]–[17] show that the spread of malware in mobile networks can be very inhomogeneous, owing primarily to the nonuniform distribution of nodes. Thus, a uniform action may be suboptimal.

We can motivate *heterogeneous* epidemics in various ways:

1) proximity-based spread, where locality causes heterogeneity;

Manuscript received April 22, 2013; revised June 25, 2014; accepted September 17, 2014; approved by IEEE/ACM TRANSACTIONS ON NETWORKING Editor S. Kasera. Date of publication November 25, 2014; date of current version February 12, 2016. This work was supported in part by the National Science Foundationunder Grant NSF:0915697. This paper was presented in part at the IEEE Information Theory and Applications Workshop (ITA), San Diego, CA, USA, February 5–10, 2012.

S. Eshghi, S. Sarkar, and S. S. Venkatesh are with the Department of Electrical and Systems Engineering, University of Pennsylvania, Philadelphia, PA 19104 USA (e-mail: eshghi@seas.upenn.edu; swati@seas.upenn.edu; venkates@seas.upenn.edu).

M. H. R. Khouzani is with the Information Security Group (ISG), Royal Holloway University of London, Egham TW20 0EX, U.K. (e-mail: arman.khouzani@rhul.ac.uk).

Color versions of one or more of the figures in this paper are available online at http://ieeexplore.ieee.org.

Digital Object Identifier 10.1109/TNET.2014.2364034

2) software/protocol diversity [18]–[20], which has even been envisioned as a defense mechanism against future threats [18];
3) IP space diversity, e.g., worms that use the IP masks of specific autonomous systems (ASs) to increase their yield [21];
4) differing clique sizes, especially for epidemics for which there is an underlying social network graph [3], [22];
5) behavioral patterns, specifically how much risky behavior every agent engages in [23];
6) clusters in cloud computing [24];
7) technology adoption, belief formation over social media, and healthcare [25]–[29].

Indeed, many works have proposed practical methods to identify, characterize, and incorporate such inhomogeneities to more accurately predict the spread of infection [2], [15], [16], [21], [30]–[33], etc. Relatively few, e.g., [3], [17], [19], and [33], consider the cost of patching and seek to minimize it in the presence of *heterogeneous contact processes*. The proposed policies in [3] and [17] are heuristic and apply to specific settings. The only papers we could find that provide *provably optimal* patching policies for *heterogeneous* networks are [19] and [33]. They, however, only consider heterogeneity in terms of infections, whereas we focus on *heterogeneity of users*. *Note that the latter involves differing contact rates across differing groups of users, which fundamentally alters the modeling and analysis*. Second, these papers only considers optimal recovery effort in their utility, while our paper optimizes recovery effort while minimizing malware damage at the same time. The optimal control of a replicative epidemic in a *heterogeneous* network is, to the best of our knowledge, without precedent. Patching performance can be significantly improved if we allow the patching rates to vary dynamically in accordance with the evolution of the infection. Characterization of the optimal controls in the space of dynamic and clustered policies has, however, so far remained elusive.

The closest work to the current paper is "Optimal energy-aware epidemic routing in DTNs" [34]. However, while these two papers both consider a *vector* of controls, the heterogeneity in the previous paper is purely due to energy, and thus the contact rates among nodes are the same (i.e., the contact process is *homogeneous*). Furthermore, the SIR epidemic model required in the current paper, as opposed to the SI model used in the previous one, fundamentally changes the nature of the interactions among nodes and therefore the nature of the optimal control problem, leading to significant changes to the analysis approach.

2) Contributions: We propose a formal framework for deriving *dynamic optimal* patching policies that leverage heterogeneity in the network structure to attain the minimum possible aggregate cost due to the spread of malware and the overhead of patching. We assume arbitrary (potentially nonlinear) functions for the cost rates of the infective nodes. We consider both *non-replicative* and *replicative* patching: In the former, some of the hosts are preloaded with the patch, which they transmit to the rest. In the latter, each recipient of the patch can also forward the patch to nodes that it contacts by a mechanism similar to the spread of the malware itself. In our model, patching can immunize susceptible nodes and may or may not heal infective nodes. The framework in each case relies on optimal control formulations that cogently capture the effect of the patching rate controls on the state dynamics and their resulting tradeoffs. We accomplish this by using a combination of damage functions associated with the controls and a *stratified*[1] mean-field deterministic epidemic model in which nodes are divided into different types. Nodes of the same type homogeneously mix with a rate specific to that type, and nodes of different types contact each other at rates particular to that pair of types. The model can therefore capture any communication topology between different groups of nodes. Above and beyond, it can exploit the inhomogeneity in the network to enable a better utilization of the resources. Such higher patching efficacy is achieved by allowing the patching controls to depend on node types, which in turn leads to *multidimensional (dynamic)* optimal control formulations.

Multidimensional optimal control formulations, particularly those in the solution space of functions rather than variables, are usually associated with the pitfall of amplifying the complexity of the optimization. An important contribution of the paper, therefore, is to prove that for both non-replicative and replicative settings the optimal control associated with each type has a simple structure provided the corresponding patching cost is either concave or convex. These structures are derived using Pontryagin's Maximum Principle and analytic arguments specific to this problem, another of our paper's contributions. This derivation reveals that the structure of the optimal control for a specific type depends only on the nature of the corresponding patching cost and not on those of other types. This holds even though the control for each type affects immunization and healing in other types and the spread of the infection in general. Specifically, if the patching cost associated with the control for a given type is concave, irrespective of the nature of the patching costs for other types, the corresponding optimal control turns out to be a bang-bang function with at most one jump: Up to a certain threshold time (possibly different for different types), it selects the maximum possible patching rate and subsequently it stops patching altogether. If the patching cost is strictly convex, the decrease from the maximum to the minimum patching rate is continuous, rather than abrupt, and monotonous. To the best of our knowledge, such simple structure results have not been established in the context of (static or dynamic) control of *heterogeneous* epidemics. Furthermore, the simplicity of these structures makes them suitable for implementation, while also providing a benchmark for other policies that may require fewer network parameters. Our numerical calculations reveal a series of interesting behaviors of optimal patching policies for different sample topologies.

To the best of our knowledge, this is the first work that considers a stratified epidemic and provides analytical structural guarantees for a dynamic patching.[2] Our model is general enough to capture any clustering of the nodes with arbitrary intercontact rates of interaction and to allow different methods of type specification. Owing to the heterogeneity of nodes, we are compelled to have differing controls for different strata

[1]Known by other terms such as structured, clustered, multiclass, multitype, multipopulation, compartmental epidemic models, and sometimes loosely as heterogeneous, inhomogeneous, or spatial epidemic models.

[2]Li *et al.* [7] consider a 2-type epidemic, but with no control. All other prior work has assumed *one uniform control* for one set of *homogeneous* users.

(types), leading to a *vector* of controls as opposed to the *single* control that was derived for *homogeneous* users in prior literature. Deriving structure results for a vector of controls requires analytical arguments that are quite different from those employed for a single control. The power of our analytical results is in the extensive generality of our model.

First, we develop our system dynamics and objectives (Section II) and characterize optimal non-replicative (Section III) and replicative (Section IV) patching. We then analyze an alternate objective (Section V) and present numerical simulation of our results (Section VI).

II. System Model and Objective Formulation

In this section, we describe and develop the model of the state dynamics of the system as a general *stratified* epidemic for both non-replicative (Section II-A) and replicative (Section II-B) patching, motivate the model (Section II-C), formulate the aggregate cost of patching, and cast this resource-aware patching as a *multidimensional* optimal control problem (Section II-E). This formulation relies on a key property of the state dynamics that we isolate in Section II-D. We develop solutions in this model framework and present our main results in Sections III and IV.

Our models are based on mean-field limits of Poisson contact processes for which pathwise convergence results have been shown (cf. [35, p. 1] and [36]).

A. Dynamics of Non-Replicative Patching

A node is *infective* if it has been contaminated by the malware, *susceptible* if it is vulnerable to the infection but not yet infected, and *recovered* if it is immune to the malware. An infective node spreads the malware to a susceptible one while transmitting data or control messages. The network consists of nodes that can be stratified into M different *types*.[3] The population of these types need not be equal. A node of type i contacts another of type j at rate $\beta_{ij}^{(N)}$.

There are $N_i = \alpha_i N$ $(\alpha_i > 0)$ nodes of type i in the network, among which $n_i^{\mathrm{S}}(t)$, $n_i^{\mathrm{I}}(t)$, and $n_i^{\mathrm{R}}(t)$ are respectively in the susceptible, infective, and recovered states at time t. Let the corresponding fractions be $S_i(t) = n_i^{\mathrm{S}}(t)/N_i$, $I_i(t) = n_i^{\mathrm{I}}(t)/N_i$, and $R_i(t) = n_i^{\mathrm{R}}(t)/N_i$. We assume that during the course of the epidemic, the populations of each type, N_i, are stable and do not change with time. Therefore, for all t and all i, we have $S_i(t) + I_i(t) + R_i(t) = 1$.

Among each type, a predetermined set of nodes, called *dispatchers*, are preloaded with the appropriate patch. Dispatchers can transmit patches to both susceptible and infective nodes, *immunizing* the susceptible and possibly *healing* the infective; in either case, successful transmission converts the target node to the recovered state. In *non-replicative* patching (as opposed to *replicative* patching—see Section II-B), the recipient nodes of the patch do not propagate it any further.[4] Dispatchers of type i contact nodes of type j at rate $\bar{\beta}_{ij}^{(N)}$, which may be different from the contact rate $\beta_{ij}^{(N)}$ of the malware between these two types. Examples where contact rates may be different include settings where the network manager may utilize a higher priority option for the distribution of patches, ones where the malware utilizes legally restricted means of propagation not available to dispatchers, or ones where the patch is not applicable to all types, with the relevant $\bar{\beta}_{ij}^{(N)}$ now being zero. The number of dispatchers of type i, which is fixed over time in the non-replicative setting, is $N_i R_i^0$, where $0 < R_i^0 < 1$.

Place the time origin $t = 0$ at the earliest moment the infection is detected and the appropriate patches generated. Suppose that at $t = 0$, for each i, an initial fraction $0 \le I_i(0) = I_i^0 \le 1$ of nodes of type i are infected. At the onset of the infection, the dispatchers $(R_i(0) = R_i^0)$ are the only agents immune to the malware. In view of node conservation, it follows that $S_i(0) = S_i^0 = 1 - I_i^0 - R_i^0$.

At any given t, any one of the $n_i^{\mathrm{S}}(t)$ susceptibles of type i may be infected by any of the $n_j^{\mathrm{I}}(t)$ infectives of type j at rate $\beta_{ji}^{(N)}$.[5] Thus, susceptibles of type i are transformed to infectives (of the same type) at an aggregate rate of $n_i^{\mathrm{S}}(t) \sum_j \beta_{ji}^{(N)} n_j^{\mathrm{I}}(t)$ by contact with infectives of any type.

The system manager regulates the resources consumed in the patch distribution by dynamically controlling the rate at which dispatchers contact susceptible and infective nodes. For each j, let the control function $u_j(t)$ represent the rate of transmission attempts of dispatchers of type j at time t. We suppose that the controls are nonnegative and bounded

$$0 \le u_j(\cdot) \le u_{j,\max}. \tag{1}$$

We will restrict consideration to control functions $u_j(\cdot)$ that have a finite number of points of discontinuity. We say that a control (vector) $\mathbf{u}(t) = (u_1(t), \ldots, u_M(t))$ is *admissible* if each $u_j(t)$ has a finite number of points of discontinuity.

Given the controls $u_1(\cdot), \ldots, u_M(\cdot)$, susceptibles of type i are transformed to recovered nodes of the same type at an aggregate rate of $n_i^{\mathrm{S}}(t) \sum_j \bar{\beta}_{ji}^{(N)} n_j^{\mathrm{R}}(0) u_j(t)$ by contact with dispatchers of any type. A subtlety in the setting is that the dispatcher may find that the efficacy of the patch is lower when treating infective nodes. This may model situations, for instance, where the malware attempts to prevent the reception or installation of the patch in an infective host, or the patch is designed only to remove the vulnerability that leaves nodes exposed to the malware but does not remove the malware itself if the node is already infected. We capture such possibilities by introducing a (type-dependent) coefficient $0 \le \pi_{ji} \le 1$, which represents the efficacy of patching an infective node: $\pi_{ji} = 0$ represents one extreme where a dispatcher of type j can only immunize susceptibles but cannot heal infectives of type i, while $\pi_{ji} = 1$ represents the other extreme where contact with a dispatcher of type j both immunizes and heals nodes of type i equally well; we also allow π_{ij} to assume intermediate values between the above extremes. An infective node transforms to the recovered state if a patch heals it; otherwise, it remains an infective. Infective nodes of type i accordingly recover at an aggregate rate of $n_i^{\mathrm{I}}(t) \sum_{j=1}^{M} \pi_{ji} \bar{\beta}_{ji}^{(N)} n_j^{\mathrm{R}}(0) u_j(t)$ by contact with dispatchers.

[3] Equivalently, *clusters, segments, populations, categories, classes, strata*.

[4] This may be preferred if the patches themselves can be contaminated and cannot be reliably authenticated.

[5] Susceptibles of type i may be contacted by infectives of type j at a higher rate, and it is possible that not all contacts lead to infection.

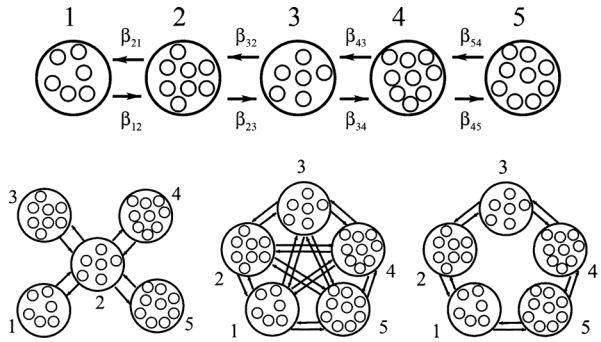

Fig. 1. Four sample topologies of five hotspot regions: linear, star, complete, and ring. For instance, nodes of hotspot 1 in the linear topology can only communicate with nodes of hotspots 1 (at rate β_{11}) and 2 (at rate β_{12}).

In the large (continuum) population regime, suppose that the two limits $\beta_{ij} := \lim_{N\to\infty} \alpha_i N \beta_{ij}^{(N)}$ and $\bar{\beta}_{ij} := \lim_{N\to\infty} \alpha_i N \bar{\beta}_{ij}^{(N)}$ exist. We say that a type j is a *neighbor* of a type i if $\beta_{ij} > 0$, and $S_j(t) > 0$ (i.e., infected nodes of type i can contact nodes of type j). There is now a natural notion of a topology that is inherited from these rates with types as vertices and edges between neighboring types. Fig. 1 illustrates some simple topologies. For a given topology inherited from the rates $\{\beta_{ij}, 1 \le i,j \le M\}$, there is now another natural notion, that of *connectivity:* We say that type j is connected to type i if, for some k, there exists a sequence of types $i = s_1 \mapsto s_2 \mapsto \cdots \mapsto s_{k-1} \mapsto s_k = j$ where type s_{l+1} is a neighbor of type s_l for $1 \le l < k$. We assume that each type is either initially infected $(I_i(0) > 0)$, or is connected to an initially infected type. We also assume that for every type i such that $R_i^0 > 0$, there exists a type j for which $\bar{\beta}_{ij} > 0$, i.e., type i can immunize nodes of at least one type, and there exist types k and l for which $\beta_{ki} > 0$ and $\beta_{il} > 0$, $S_l(0) > 0$, i.e., the infection can spread to and from that type. (In most settings, we may expect, naturally, that $\beta_{ii} > 0$ and $\bar{\beta}_{ii} > 0$.)

Thus, we have[6]

$$\dot{S}_i = -\sum_{j=1}^{M} \beta_{ji} I_j S_i - S_i \sum_{j=1}^{M} \bar{\beta}_{ji} R_j^0 u_j \tag{2a}$$

$$\dot{I}_i = \sum_{j=1}^{M} \beta_{ji} I_j S_i - I_i \sum_{j=1}^{M} \pi_{ji} \bar{\beta}_{ji} R_j^0 u_j \tag{2b}$$

where, by writing $\mathbf{S}(t) = (S_1(t), \ldots, S_M(t))$, $\mathbf{I}(t) = (I_1(t), \ldots, I_M(t))$, and $\mathbf{R}^0(t) = (R_1^0(t), \ldots, R_M^0(t))$ in a compact vector notation, the initial conditions and state constraints are given by

$$\mathbf{S}(0) = \mathbf{S}^0 \succeq \mathbf{0} \quad \mathbf{I}(0) = \mathbf{I}^0 \succeq \mathbf{0} \tag{3}$$

$$\mathbf{S}(t) \succeq \mathbf{0} \quad \mathbf{I}(t) \succeq \mathbf{0} \quad \mathbf{S}(t) + \mathbf{I}(t) \preceq \mathbf{1} - \mathbf{R}^0. \tag{4}$$

In these expressions, $\mathbf{0}$ and $\mathbf{1}$ represent vectors all of whose components are 0 and 1, respectively, and the vector inequalities are to be interpreted as component-wise inequalities. Note that the evolution of $\mathbf{R}(t)$ need not be explicitly considered since at any given time, node conservation gives $R_i(t) = 1 - S_i(t) - I_i(t)$. We henceforth drop the dependence on t and make it implicit whenever we can do so without ambiguity.

[6]We use dots to denote *time* derivatives throughout, e.g., $\dot{S}(t) = dS(t)/dt$.

B. Dynamics of Replicative Patching

In the replicative setting, a recipient of the patch can forward it to other nodes upon subsequent contact. Thus, recovered nodes of type i are added to the pool of dispatchers of type i, whence the fraction of dispatchers of type i grows from the initial $R_i(0) = R_i^0$ to $R_i(t)$ at time t. This should be contrasted with the non-replicative model in which the fraction of dispatchers of type i is fixed at R_i^0 for all t.

The system dynamics equations given in (2) for the non-replicative setting now need to be modified to take into account the growing pool of dispatchers. While in the non-replicative case we chose the pair $(\mathbf{S}(t), \mathbf{I}(t))$ to represent the system state, in the replicative case it is slightly more convenient to represent the system state by the explicit triple $(\mathbf{S}(t), \mathbf{I}(t), \mathbf{R}(t))$. The system dynamics are now governed by

$$\dot{S}_i = -\sum_{j=1}^{M} \beta_{ji} I_j S_i - S_i \sum_{j=1}^{M} \bar{\beta}_{ji} R_j u_j \tag{5a}$$

$$\dot{I}_i = \sum_{j=1}^{M} \beta_{ji} I_j S_i - I_i \sum_{j=1}^{M} \pi_{ji} \bar{\beta}_{ji} R_j u_j \tag{5b}$$

$$\dot{R}_i = S_i \sum_{j=1}^{M} \bar{\beta}_{ji} R_j u_j + I_i \sum_{j=1}^{M} \pi_{ji} \bar{\beta}_{ji} R_j u_j \tag{5c}$$

with initial conditions and state constraints given by

$$\mathbf{S}(0) = \mathbf{S}^0 \succeq \mathbf{0} \quad \mathbf{I}(0) = \mathbf{I}^0 \succeq \mathbf{0} \quad \mathbf{R}(0) = \mathbf{R}^0 \succeq \mathbf{0} \tag{6}$$

$$\mathbf{S}(t) \succeq \mathbf{0} \quad \mathbf{I}(t) \succeq \mathbf{0} \quad \mathbf{R}(t) \succeq \mathbf{0} \quad \mathbf{S}(t) + \mathbf{I}(t) + \mathbf{R}(t) = \mathbf{1}. \tag{7}$$

The assumptions on controls and connectivity are as in Section II-A.

C. Motivation of the Models and Instantiations

We now motivate the stratified epidemic models (2) and (5) through examples, instantiating the types in each context.

1) Proximity-Based Spread—Heterogeneity Through Locality: The overall roaming area of the nodes can be divided into regions (e.g., hotspots, office/residential areas, central/peripheral areas, etc.) of different densities (Fig. 1). One can therefore stratify the nodes based on their locality, i.e., each type corresponds to a region. IP eavesdropping techniques (using software such as `AirJack`, `Ethereal`, `FakeAP`, `Kismet`, etc.) allow malware to detect new victims in the vicinity of the host. Distant nodes have more attenuated signal strength [i.e., lower signal-to-interference-plus-noise ratio (SINR)] and are therefore less likely to be detected. Accordingly, malware (and also patch) propagation rates β_{ij} (respectively, $\bar{\beta}_{ij}$) are related to the local densities of the nodes in each region and decay with an increase in the distance between regions i and j: Typically, β_{ii} exceeds β_{ij} for $i \neq j$, likewise for $\bar{\beta}_{ij}$. The same phenomenon was observed for malware such as `cabir` and `lasco` that use Bluetooth and Infrared to propagate.

2) Heterogeneity Through Software/Protocol Diversity: A network that relies on a homogeneous software/protocol is vulnerable to an attack that exploits a common weakness (e.g.,

a buffer overflow vulnerability). Accordingly, inspired by the natural observation that *the chances of survival are improved by heterogeneity*, increasing the network's heterogeneity without sacrificing interoperability has been proposed as a defense mechanism [18]. In practice, mobile nodes use different operating systems and communication protocols, e.g., `Symbian`, `Android`, `iOS`, `RIM`, `webOS`, etc. Such heterogeneities lead to dissimilar rates of propagation of malware among different types, where each type represents a specific OS, platform, software, protocol, etc. In the extreme case, the malware may not be able to contaminate nodes of certain types. The patching response should take such inhomogeneities into account in order to optimally utilize network resources since the rate of patching can also be dissimilar among different types.

3) Heterogeneity Through Available IP Space: Smartphone trojans like `skulls` and `mosquito` spread using Internet or P2P networks. In such cases, the network can be decomposed into ASs, with each type representing an AS [21]. A worm either scans IP addresses uniformly randomly or uses the IP masks of ASs to restrict its search domain and increase its rate of finding new susceptible nodes. In each of these cases, the contact rates differ between different ASs depending on the actual number of assigned IPs in each IP subdomain and the maximum size of that IP subdomain.

4) Heterogeneity Through Differing Clique Sizes: Malware that specifically spreads in social networks has been recorded in the past few years [22]. Examples include `Samy` in MySpace in 2005 and `Koobface` in MySpace and Facebook in 2008. `Koobface`, for instance, spread by delivering (contaminated) messages to the "friends" of an infective user. MMS-based malware such as `commwarrior` can also utilize the contact list of an infective host to access new handsets. In such cases, the social network graph can be approximated by a collection of friendship *cliques*.[7] Users of the same clique can be regarded as the same type with the rate of contact within cliques and across cliques differing depending on the relative sizes of the cliques.[8]

5) Cloud Computing—Heterogeneity Through Cluster Sizes: In cluster (or grid or volunteer) computing [24], each cluster of CPUs in the cloud constitutes a type. Any two computers in the same cluster can communicate at faster rates than those in different clusters. These contact rates depend on the communication capacity of connecting lines as well as the relative number of computers in each cluster.

6) Clustered Epidemics in Technology Adoption, Belief Formation Over Social Media, and Healthcare: We now elaborate on the application of our clustered epidemics model in these diverse set of contexts. First, consider a rivalry between two technologies or companies for adoption in a given population, e.g., Android and iPhone or cable and satellite television. Individuals who are yet to choose either may be considered as susceptibles, and those who have chosen one or the other technology would be classified as either infective or recovered depending upon their choice. Dispatchers constitute the promoters of a given technology (the one whose subscribers are denoted as recovered). Awareness about the technology and subsequent subscription to either may spread through social contact between infectives and susceptibles (infection propagation in our terminology), and dispatchers and the rest (patching in our terminology). Immunization of a susceptible corresponds to her adoption of the corresponding technology, while healing of an infective corresponds to an alteration in her original choice. The stratifications may be based on location or social cliques, and the control $\mathbf{u}$ would represent promotion efforts, which would be judiciously selected by the proponent of the corresponding technology. Patching may either be replicative or non-replicative depending on whether the newly subscribed users are enticed to attract more subscribers by referral rewards. Similarly, clustered epidemics may be used to model belief management over social media, where infective and recovered nodes represent individuals who have conflicting persuasions, and susceptibles represent those who are yet to subscribe to either doctrine. Last but not least, the susceptible-infective-recovered classification and immunization/healing/infection have natural connotations in the context of a biological epidemic. Here, the dispatchers correspond to health workers who administer vaccines and/or hospitalization, and the stratification is based on location. Note that in this context, patching can only be non-replicative.

D. Key Observations

A natural but important observation is that if the initial conditions are nonnegative, then the system dynamics (2) and (5) yield unique states satisfying the positivity and normalization constraints (4) and (7), respectively. The proof is technical and is not needed elsewhere in the paper; we relegate it accordingly to the Appendix.

Theorem 1: The dynamical system (2) [respectively (5)] with initial conditions (3) [respectively, (6)] has a unique state solution $(\mathbf{S}(t), \mathbf{I}(t))$ [respectively $(\mathbf{S}(t), \mathbf{I}(t), \mathbf{R}(t))$] that satisfies the state constraints (4) [respectively, (7)]. For all $t > 0$, $I_i(t) > 0$; $R_i(t) > 0$ if $R_i(0) > 0$; and $S_j(t) > 0$ if and only if $S_j(0) \neq 0$. For each j such that $S_j(0) = 0$, $S_j(t') = 0$ for all $t' \in (0, T]$.

E. Optimality Objective

The network seeks to minimize the overall cost of infection and the resource overhead of patching in a given operation time window $[0, T]$. At any given time t, the system incurs costs at a rate $f(\mathbf{I}(t))$ due to the malicious activities of the malware.[9] For instance, the malware may use infected hosts to eavesdrop, analyze, misroute, alter, or destroy the traffic that the hosts generate or relay. We suppose that $f(\mathbf{0}) = 0$ and make the natural assumption that the scalar function $f(\mathbf{I})$ is increasing and differentiable with respect to each I_i. The simplest natural candidate for $f(\mathbf{I})$ is of the form $\sum_{i=1}^{M} f_i(I_i)$; in this setting, each f_i is a nondecreasing function of its argument representing the cost

[7] A clique is a maximal complete subgraph of a graph [37, p. 112].

[8] In MMS/e-mail, types typically depend on the nature of social contact, while in Bluetooth, types are naturally based on distance to the center of the cluster, as nodes that are closer are more likely to contact each other. Wang *et al.* [2] examine the spreading patterns of viruses through both these mechanisms with the same assumption as our paper in terms of the underlying variable behind the spread (proximity for Bluetooth and social ties for MMS). Furthermore, our model is general enough to even capture the hybrid spread of a virus that the authors investigate. In that case, the types would be based on both distance to the center of the cluster *and* the nature of the social contact.

[9] This is a standard assumption in the field of epidemics, e.g., Rowthorn *et al.* [38] and Sethi and Staats [39])

of infection for type i, which is in turn determined by the criticality of the data of that type and its function.[10] The network also benefits at the rate of $L(\mathbf{R}(t))$, i.e., incurs a cost at the rate of $-L(\mathbf{R}(t))$, due to the removal of uncertainty about the state of the nodes being patched. The inclusion of $L(\mathbf{R})$ allows the framework to capture domains such as belief propagation and technology adoption, where there are gains associated with the fraction of recovered nodes at each instant. We suppose that the scalar function $L(\mathbf{R})$ is nondecreasing and differentiable with respect to each R_i (e.g., allowing constant or zero functions).

In addition to the cost of infection, each dispatcher burdens the network with a cost by consuming either available bandwidth, energy reserves of the nodes (e.g., in communication and computing networks), or money (e.g., in technology adoption, propaganda, health-care) to disseminate the patches. Suppose dispatchers of type i incur cost at a rate of $R_i^0 h_i(u_i)$. We suppose that the overhead of extra resource (bandwidth or energy or money) consumption at time t is then given by a sum of the form $\sum_{i=1}^{M} R_i^0 h_i(u_i)$. The scalar functions $h_i(\cdot)$ represent how much resource is consumed for transmission of the patch by nodes of each type and how significant this extra taxation of resources is for each type. Naturally enough, we assume these functions are nondecreasing and satisfy $h_i(0) = 0$ and $h_i(\gamma) > 0$ for $\gamma > 0$. We assume, additionally, that each h_i is twice differentiable. Following the same lines of reasoning, the corresponding expression for the cost of replicative patching is of the form $\sum_{i=1}^{M} R_i h_i(u_i)$. In problems that arise from the field of computer networks, such as malware propagation and cloud computing, we would expect to have concave $h_i(\cdot)$, as the marginal effort required to spread the epidemic at a contact opportunity would be expected to rise negligibly. For example, in a delay-tolerant network, every contact between a transmitting recovered and another node would already involve beaconing and the exchange of messages that identify the state of the nodes, and transmitting the patch more frequently would just affect the part of the transmission cost that is to do with the patch itself. However, when looking at social networks, for example, asking a user to spread a message more often can lead to reluctance on its part, and this would justify $h_i(\cdot)$ that are convex. We therefore allow for both convex and concave $h_i(\cdot)$ functions.

With the arguments stated above, the aggregate cost for non-replicative patching is given by an expression of the form

$$J_{\text{non-rep}} = \int_0^T \left(f(\mathbf{I}) - L(\mathbf{R}) + \sum_{i=1}^{M} R_i^0 h_i(u_i) \right) dt \qquad (8)$$

while for replicative patching, the aggregate cost is of the form

$$J_{\text{rep}} = \int_0^T \left(f(\mathbf{I}) - L(\mathbf{R}) + \sum_{i=1}^{M} R_i h_i(u_i) \right) dt. \qquad (9)$$

Problem Statement: The system seeks to minimize the aggregate cost (**A**) in (8) for non-replicative patching [(2) and (3)] and (**B**) in (9) for replicative patching [(5) and (6)] by an appropriate selection of an optimal admissible control $\mathbf{u}(t)$. In this setting, it is clear that by a scaling of $\bar{\beta}_{ji}$ and $h_j(\cdot)$, we can assume WLoG that $u_{j,\max} = 1$.

[10]Such differences themselves may be a source of stratification. In general, different types need not exclusively reflect disparate mixing rates.

It is worth noting that any control in the non-replicative case can be emulated in the replicative setting: This is because the fraction of the dispatchers in the replicative setting is nondecreasing, hence at any time instance, a feasible $u^{\text{rep}}(t)$ can be selected such that $R_i(t)u_i^{\text{rep}}(t)$ is equal to $R_i^0 u_i^{\text{non-rep}}(t)$. This means that the minimum cost of replicative patching is always less than the minimum cost of its non-replicative counterpart. Our numerical results will show that this improvement is substantial. However, replicative patches increase the risk of patch contamination: The security of a smaller set of known dispatchers is easier to manage than that of a growing set whose identities may be ambiguous. Hence, in a nutshell, if there is a dependable mechanism for authenticating patches, replicative patching ought to be the preferred method, otherwise one needs to evaluate the tradeoff between the risk of compromised patches and the efficiency of the patching.

III. Optimal Non-Replicative Patching

A. Numerical Framework for Computing the Optimal Controls

The main challenge in computing the optimal state and control functions $((\mathbf{S}, \mathbf{I}), \mathbf{u})$ is that while the differential equations (2) can be solved once the optimal controls $\mathbf{u}(\cdot)$ are known, an exhaustive search for an optimal control is infeasible as there are an uncountably infinite number of control functions. *Pontryagin's Maximum Principle* (PMP) provides an elegant technique for solving this seemingly intractable problem (cf. [40]). Referring to the integrand in (8) as $\xi_{\text{non-rep}}$ and the right-hand side (RHS) of (2a) and (2b) as ν_i and μ_i, we define the Hamiltonian to be

$$\mathcal{H} = \mathcal{H}(\mathbf{u}) := \xi_{\text{non-rep}} + \sum_{i=1}^{M} \left(\lambda_i^{\text{S}} \nu_i + \lambda_i^{\text{I}} \mu_i \right) \qquad (10)$$

where the *adjoint* (or *costate*) functions λ_i^{S} and λ_i^{I} are continuous functions that for each $i = 1 \ldots M$, and at each point of continuity of $\mathbf{u}(\cdot)$, satisfy

$$\dot{\lambda}_i^{\text{S}} = -\frac{\partial \mathcal{H}}{\partial S_i} \quad \dot{\lambda}_i^{\text{I}} = -\frac{\partial \mathcal{H}}{\partial I_i} \qquad (11)$$

along with the final (i.e., transversality) conditions

$$\lambda_i^S(T) = 0 \quad \lambda_i^I(T) = 0. \qquad (12)$$

Then, PMP implies that the optimal control at time t satisfies

$$\mathbf{u} \in \arg\min_{\mathbf{v}} \mathcal{H}(\mathbf{v}) \qquad (13)$$

where the minimization is over the space of admissible controls (i.e., $H(u) = \min_v H(v)$).

In economic terms, the adjoint functions represent a shadow price (or imputed value); they measure the marginal worth of an increment in the state at time t when moving along an optimal trajectory. Intuitively, in these terms, λ_i^{I} ought to be positive as it represents the additional cost that the system incurs per unit time with an increase in the fraction of infective nodes. Furthermore, as an increase in the fraction of the infective nodes has worse long-term implications for the system than an increase in the fraction of the susceptibles, we anticipate that $\lambda_i^{\text{I}} - \lambda_i^{\text{S}} > 0$. The following result confirms this intuition. It is of value in its own right, but as its utility for our purposes is in the proof of our

main theorem of the following section, we will defer its proof (to Section III-C) to avoid breaking up the flow of the narrative at this point.

Lemma 1: The positivity constraints $\lambda_i^{\mathrm{I}}(t) > 0$ and $\lambda_i^{\mathrm{I}}(t) - \lambda_i^{\mathrm{S}}(t) > 0$ hold for all $i = 1, \ldots, M$ and all $t \in [0, T)$.

The abstract maximum principle takes on a very simple form in our context. Using the expression for $\xi_{\text{non-rep}}$ from (8) and the expressions for ν_i and μ_i from (2), trite manipulations show that the minimization (13) may be expressed in the much simpler (nested) scalar formulation

$$u_i(t) \in \arg\min_{0 \le x \le 1} \psi_i(x, t) \qquad (1 \le i \le M) \tag{14}$$

$$\psi_i(x, t) := R_i^0 (h_i(x) - \phi_i(t) x) \tag{15}$$

$$\phi_i := \sum_{j=1}^{M} \bar{\beta}_{ij} \lambda_j^{\mathrm{S}} S_j + \sum_{j=1}^{M} \bar{\beta}_{ij} \pi_{ij} \lambda_j^{\mathrm{I}} I_j. \tag{16}$$

Equation (14) allows us to characterize u_i as a function of the state and adjoint functions at each time instant. Plugging into (2) and (11), we obtain a system of (nonlinear) differential equations that involves only the state and adjoint functions (and not the control $\mathbf{u}(\cdot)$), and where the initial values of the states (3) and the final values of the adjoint functions (12) are known. Numerical methods for solving *boundary value* nonlinear differential equation problems may now be used to solve for the state and adjoint functions corresponding to the optimal control, thus providing the optimal controls using (14).

We conclude this section by proving an important property of $\phi_i(\cdot)$, which we will use in subsequent sections.

Lemma 2: For each i, $\phi_i(t)$ is a decreasing function of t.

Proof: We examine the derivative of $\phi_i(t)$; we need expressions for the derivatives of the adjoint functions toward that end. From (10) and (11), at any t at which $\mathbf{u}$ is continuous, we have

$$\begin{aligned}
\dot{\lambda}_i^{\mathrm{S}} &= -\frac{\partial L(\mathbf{R})}{\partial R_i} - \left(\lambda_i^{\mathrm{I}} - \lambda_i^{\mathrm{S}}\right) \sum_{j=1}^{M} \beta_{ji} I_j + \lambda_i^{\mathrm{S}} \sum_{j=1}^{M} \bar{\beta}_{ji} R_j^0 u_j \\
\dot{\lambda}_i^{\mathrm{I}} &= -\sum_{j=1}^{M} \left(\left(\lambda_j^{\mathrm{I}} - \lambda_j^{\mathrm{S}}\right) \beta_{ij} S_j\right) + \lambda_i^{\mathrm{I}} \sum_{j=1}^{M} \pi_{ji} \bar{\beta}_{ji} R_j^0 u_j \\
&\quad - \frac{\partial L(\mathbf{R})}{\partial R_i} - \frac{\partial f(\mathbf{I})}{\partial I_i}.
\end{aligned} \tag{17}$$

Using (16), (17), and some reassembly of terms, at any t at which $\mathbf{u}$ is continuous, $\dot{\phi}_i(t) = -\sum_{j=1}^{M} \bar{\beta}_{ij} [S_j \frac{\partial L(\mathbf{R})}{\partial R_j} + \pi_{ij} I_j (\frac{\partial L(\mathbf{R})}{\partial R_j} + \frac{\partial f(\mathbf{I})}{\partial I_j}) + \sum_{k=1}^{M} (1 + \pi_{ij}) \lambda_j^{\mathrm{I}} \beta_{kj} S_j I_k + \sum_{k=1}^{M} \pi_{ij} I_j S_k \beta_{jk} (\lambda_k^{\mathrm{I}} - \lambda_k^{\mathrm{S}})]$. The assumptions on $L(\cdot)$ and $f(\cdot)$ (together with Theorem 1) show that the first two terms inside the square brackets on the right are always nonnegative. Theorem 1 and Lemma 1 (together with our assumptions on π_{ij}, β_{ij}, and $\bar{\beta}_{ij}$) show that the penultimate term is positive for $t > 0$ and the final term is nonnegative. It follows that $\dot{\phi}_i(t) < 0$ for every $t \in (0, T)$ at which $\mathbf{u}(t)$ is continuous. As $\phi_i(t)$ is a continuous function of time and its derivative is negative except at a finite number of points (where $\mathbf{u}$ may be discontinuous), it follows indeed that, as advertised, $\phi_i(t)$ is a decreasing function of time. □

B. Structure of Optimal Non-Replicative Patching

We are now ready to identify the structure of the optimal control $(u_1(t), \ldots, u_M(t))$:

Theorem 2: Predicated on the existence of an optimal control, for types i such that $R_i^0 > 0$: If $h_i(\cdot)$ is concave, then the optimal control for type i has the following structure: $u_i(t) = 1$ for $0 < t < t_i$, and $u_i(t) = 0$ for $t_i < t \le T$, where $t_i \in [0, T)$. If $h_i(\cdot)$ is strictly convex, then the optimal control for type i, $u_i(t)$ is continuous and has the following structure: $u_i(t) = 1$ for $0 < t < t_i^1$, $u_i(t) = 0$ for $t_i^2 < t \le T$, and $u_i(t)$ strictly decreases in the interval $[t_i^1, t_i^2]$, where $0 \le t_i^1 < t_i^2 \le T$.

Notice that if $R_i^0 = 0$ in (2), the control u_i is irrelevant and can take any arbitrary admissible value. Intuitively, at the onset of the epidemic, a large fraction of nodes are susceptible to the malware ("potential victims"). Bandwidth and power resources should hence be used maximally in the beginning (in all types), rendering as many infective and susceptible nodes robust against the malware as possible. In particular, there is no gain in deferring patching since the efficacy of healing infective nodes is less than that of immunizing susceptible nodes (recall that $\pi_{ij} \le 1$). While the nonincreasing nature of the optimal control is intuitive, what is less apparent is the characteristics of the decrease, which we establish in this theorem. For concave $h_i(\cdot)$, nodes are patched at the maximum possible rate until a time instant when patching stops abruptly, while for strictly convex $h_i(\cdot)$, this decrease is continuous. It is instructive to note that the structure of the optimal action taken by a type only depends on its own patching cost and not on that of its neighbors. This is somewhat counterintuitive as the controls for one type affect the infection and recovery of other types. The timing of the decrease in each type differs and depends on the location of the initial infection as well as the topology of the network, communication rates, etc.

Proof: For nonlinear concave $h_i(\cdot)$, (14) requires the minimization of the (nonlinear concave) difference between a nonlinear concave function of a scalar variable x and a linear function of x at all time instants; hence, the minimum can only occur at the endpoints of the interval over which x can vary. Thus, all that needs to be done is to compare the values of $\psi_i(x, t)$ for the following two candidates: $x = 0$ and $x = 1$. Note that $\psi_i(0, t) = 0$ at all time instants and $\psi_i(1, t)$ is a function of time t. Let

$$\gamma_i(t) := \psi_i(1, t) = R_i^0 h_i(1) - R_i^0 \phi_i(t). \tag{18}$$

Then, the optimal u_i satisfies the following condition:

$$u_i(t) = \begin{cases} 1, & \gamma_i(t) < 0 \\ 0, & \gamma_i(t) > 0. \end{cases} \tag{19}$$

From the transversality conditions in (12) and the definition of $\phi_i(t)$ in (16), for all i, it follows that $\phi_i(T) = 0$. From the definition of the cost term, $h_i(1) > 0$, hence, since $R_i^0 > 0$, therefore $\gamma_i(T) > 0$. Thus, the structure of the optimal control predicted in the theorem for the strictly concave case will follow from (19) if we can show that $\gamma_i(t)$ is an increasing function of time t, as that implies that it can be zero at most at one point t_i, with $\gamma_i(t) < 0$ for $t < t_i$ and $\gamma_i(t) > 0$ for $t > t_i$. From (18), γ_i will be an increasing function of time if ϕ_i is a decreasing function of time, a property that we showed in Lemma 2.

If $h_i(\cdot)$ is linear (i.e., $h_i(x) = K_i x, K_i > 0$, since $h_i(x) > 0$ for $x > 0$), $\psi_i(x,t) = R_i^0 x(K_i - \phi_i(t))$, and from (14), the condition for an optimal u_i is

$$u_i(t) = \begin{cases} 1, & \phi_i(t) > K_i \\ 0, & \phi_i(t) < K_i. \end{cases} \tag{20}$$

However, from (12), $\phi_i(T) = 0 < K_i$, and as by Lemma 2, $\phi_i(t)$ is decreasing, it follows that $\phi_i(t)$ will be equal to K_i at most at one time instant $t = t_i$, with $\phi_i(t) > 0$ for $t < t_i$ and $\phi_i(t) < 0$ for $t > t_i$. This, along with (20), concludes the proof of the theorem for the concave case.

We now consider the case where $h_i(\cdot)$ is strictly convex. In this case, the minimization in (14) may also be attained at an interior point of $[0,1]$ (besides 0 and 1) at which the partial derivative of the right-hand side with respect to x is zero. Hence

$$u_i(t) = \begin{cases} 1, & 1 < \eta(t) \\ \eta(t), & 0 < \eta(t) \le 1 \\ 0, & \eta(t) \le 0. \end{cases} \tag{21}$$

where $\eta(t)$ is such that $\frac{dh_i(x)}{dx}|_{(x=\eta(t))} = \phi_i(t)$.

Note that $\phi_i(t)$ is a continuous function due to the continuity of the states and adjoint functions. We showed that it is also a decreasing function of time (Lemma 2). Since $h_i(\cdot)$ is double differentiable, its first derivative is continuous, and since it is strictly convex, its derivative is a strictly increasing function of its argument. Therefore, $\eta(t)$ must be a continuous and decreasing function of time, as per the predicted structure. □

C. Proof of Lemma 1

Proof: From (17) and (12), at time T, we have

$$\begin{aligned} \lambda_i^{\mathrm{I}}|_{t=T} &= \left(\lambda_i^{\mathrm{I}} - \lambda_i^{\mathrm{S}}\right)\big|_{t=T} = 0 \\ \lim_{t\uparrow T} \dot{\lambda}_i^{\mathrm{I}} &= -\frac{\partial L(\mathbf{R})}{\partial R_i}(T) - \frac{\partial f(\mathbf{I})}{\partial I_i}(T) < 0 \\ \lim_{t\uparrow T} \left(\dot{\lambda}_i^{\mathrm{I}} - \dot{\lambda}_i^{\mathrm{S}}\right) &= -\frac{\partial f(\mathbf{I})}{\partial I_i}(T) < 0. \end{aligned}$$

Hence, $\exists \epsilon > 0$ s.t. $\lambda_i^{\mathrm{I}} > 0$ and $(\lambda_i^{\mathrm{I}} - \lambda_i^{\mathrm{S}}) > 0$ over $(T-\epsilon, T)$.

Now suppose that, going backward in time from $t = T$, (at least) one of the inequalities is first violated at $t = t^*$ for i^*, i.e., for all i, $\lambda_i^{\mathrm{I}}(t) > 0$ and $(\lambda_i^{\mathrm{I}}(t) - \lambda_i^{\mathrm{S}}(t)) > 0$ for all $t > t^*$ and either: A) $(\lambda_{i^*}^{\mathrm{I}}(t^*) - \lambda_{i^*}^{\mathrm{S}}(t^*)) = 0$; or B) $\lambda_{i^*}^{\mathrm{I}}(t^*) = 0$ for some $i = i^*$. Note that from continuity of the adjoint functions, $\lambda_i^{\mathrm{I}}(t^*) \ge 0$ and $(\lambda_i^{\mathrm{I}}(t^*) - \lambda_i^{\mathrm{S}}(t^*)) \ge 0$ for all i.

We investigate Case A first. We have:[11] $(\dot{\lambda}_{i^*}^{\mathrm{I}} - \dot{\lambda}_{i^*}^{\mathrm{S}})(t^{*+}) = -\frac{\partial f(\mathbf{I})}{\partial I_{i^*}} - \sum_{j=1}^{M}[(\lambda_j^{\mathrm{I}} - \lambda_j^{\mathrm{S}})\beta_{i^*j}S_j] - \lambda_{i^*}^{\mathrm{I}}\sum_{j=1}^{M}\bar{\beta}_{ji^*}(1 - \pi_{ji^*})R_j^0 u_j$. First of all, $-\partial f(\mathbf{I})/\partial I_{i^*} < 0$. The other two terms are nonpositive due to the definition of t^* and $\pi_{ij} \le 1$. Hence, $(\dot{\lambda}_{i^*}^{\mathrm{I}} - \dot{\lambda}_{i^*}^{\mathrm{S}})(t^{*+}) < 0$, which is in contradiction with Property 1 of real-valued functions, proved in [8].

Property 1: Let $g(t)$ be a continuous and piecewise differentiable function of t. If $g(t_0) = L$ and $g(t) > L$ ($g(t) < L$) for all $t \in (t_0, t_1]$. Then, $\dot{g}(t_0^+) \ge 0$ (respectively, $\dot{g}(t_0^+) \le 0$).

On the other hand, for Case B, we have:[11] $\dot{\lambda}_{i^*}^{\mathrm{I}}(t^{*+}) = -\frac{\partial L(\mathbf{R})}{\partial R_{i^*}} - \frac{\partial f(\mathbf{I})}{\partial I_{i^*}} - \sum_{j=1}^{M}[(\lambda_j^{\mathrm{I}} - \lambda_j^{\mathrm{S}})\beta_{i^*j}S_j]$, which is negative since $-\partial L(\mathbf{R})/\partial R_{i^*} \le 0$, $-\partial f(\mathbf{I})/\partial I_{i^*} < 0$, and from the definition of t^* (for the third term). This contradicts Property 1, and the claim follows. □

[11] $g(t_0^+) := \lim_{t\downarrow t_0} g(t)$ and $g(t_0^-) := \lim_{t\uparrow t_0} g(t)$. The RHS of the equation is evaluated at $t = t^*$ due to continuity.

IV. Optimal Replicative Patching

A. Numerical Framework for Computing the Optimal Controls

As in the non-replicative setting, we develop a numerical framework for calculation of the optimal solutions using PMP, and then we establish the structure of the optimal controls.

For every control $\tilde{\mathbf{u}}$, we define $\tau_i(\mathbf{I}(0), \mathbf{S}(0), \mathbf{R}(0), \tilde{\mathbf{u}}) \in [0,T]$ as follows: If $R_i(0) > 0$, and therefore $R_i(t) > 0$ for all $t > 0$ due to Theorem 1, we define $\tau_i(\mathbf{I}(0), \mathbf{S}(0), \mathbf{R}(0), \tilde{\mathbf{u}})$ to be 0. Else, $\tau_i(\mathbf{I}(0), \mathbf{S}(0), \mathbf{R}(0), \tilde{\mathbf{u}})$ is the maximum t for which $R_i(t) = 0$. It follows from Theorem 1 that $R_i(t) = 0$ for all $t \le \tau_i(\mathbf{I}(0), \mathbf{S}(0), \mathbf{R}(0), \tilde{\mathbf{u}})$ and all i such that $R_i(0) = 0$, and $R_i(t) > 0$ for all $\tau_i(\mathbf{I}(0), \mathbf{S}(0), \mathbf{R}(0), \tilde{\mathbf{u}}) < t \le T$. We begin with the hypothesis that there exists at least one optimal control, say $\tilde{\mathbf{u}} \in \mathcal{U}^*$, and construct a control $\mathbf{u}$ that chooses $u_i(t) := 0$ for $t \le \tau_i(\mathbf{I}(0), \mathbf{S}(0), \mathbf{R}(0), \tilde{\mathbf{u}})$ and $u_i(t) := \tilde{u}_i(t)$ for $t > \tau_i(\mathbf{I}(0), \mathbf{S}(0), \mathbf{R}(0), \tilde{\mathbf{u}})$. Clearly, the states $\mathbf{S}(t), \mathbf{I}(t), \mathbf{R}(t)$ corresponding to $\tilde{\mathbf{u}}$ also constitute the state functions for $\mathbf{u}$, as the state equations only differ at $t = 0$, a set of measure zero. Thus, $\mathbf{u}$ is also an optimal control, and $\tau_i(\mathbf{I}(0), \mathbf{S}(0), \mathbf{R}(0), \tilde{\mathbf{u}}) = \tau_i(\mathbf{I}(0), \mathbf{S}(0), \mathbf{R}(0), \mathbf{u})$ for each i. Henceforth, for notational convenience, we will refer to $\tau_i(\mathbf{I}(0), \mathbf{S}(0), \mathbf{R}(0), \tilde{\mathbf{u}}), \tau_i(\mathbf{I}(0), \mathbf{S}(0), \mathbf{R}(0), \mathbf{u})$ as τ_i. Note that the definition of this control completely specifies the values of each u_i in $[0,T]$.

Referring to the integrand of (9) as ξ_{rep} and the RHS of (5a)–(5c) as ν_i, μ_i, and ρ_i, the Hamiltonian becomes

$$\mathcal{H} = \mathcal{H}(\mathbf{u}) := \xi_{\mathrm{rep}} + \sum_{i=1}^{M}\left[\left(\lambda_i^{\mathrm{S}}\nu_i + \lambda_i^{\mathrm{I}}\mu_i + \lambda_i^{\mathrm{R}}\rho_i\right)\right. \tag{22}$$

where the *adjoint* functions $\lambda_i^{\mathrm{S}}, \lambda_i^{\mathrm{I}}, \lambda_i^{\mathrm{R}}$ are continuous functions that at each point of continuity of $\mathbf{u}(\cdot)$ and for all $i = 1 \ldots M$ satisfy

$$\dot{\lambda}_i^{\mathrm{S}} = -\frac{\partial \mathcal{H}}{\partial S_i} \quad \dot{\lambda}_i^{\mathrm{I}} = -\frac{\partial \mathcal{H}}{\partial I_i} \quad \dot{\lambda}_i^{\mathrm{R}} = -\frac{\partial \mathcal{H}}{\partial R_i} \tag{23}$$

with the final constraints

$$\lambda_i^{\mathrm{S}}(T) = \lambda_i^{\mathrm{I}}(T) = \lambda_i^{\mathrm{R}}(T) = 0. \tag{24}$$

According to PMP, any optimal controller must satisfy

$$\mathbf{u} \in \arg\min_{\mathbf{v}} \mathcal{H}(\mathbf{v}) \tag{25}$$

where the minimization is over the set of admissible controls.

Using the expressions for ξ_{rep} from (9) and the expressions for ν_i, μ_i, and ρ_i from (5), it can be shown that the vector minimization (25) can be expressed as a scalar minimization

$$u_i(t) \in \arg\min_{0\le x\le 1} \psi_i(x,t) \qquad (1 \le i \le M) \tag{26}$$

$$\psi_i(x,t) := R_i(t)(h_i(x) - \phi_i(t)x) \tag{27}$$

$$\phi_i := \sum_{j=1}^{M} \bar{\beta}_{ij}\left(\lambda_j^{\mathrm{S}} - \lambda_j^{\mathrm{R}}\right) S_j + \sum_{j=1}^{M} \pi_{ij}\bar{\beta}_{ij}\left(\lambda_j^{\mathrm{I}} - \lambda_j^{\mathrm{R}}\right) I_j. \tag{28}$$

Equation (26) characterizes the optimal control u_i as a function of the state and adjoint functions at each instant. Plugging the optimal u_i into the state and adjoint function equations [respectively, (5) and (23)] will again leave us with a system of (nonlinear) differential equations that involves only the state and adjoint functions (and not the control $\mathbf{u}(\cdot)$), the initial values of the states (6), and the final values of the adjoint functions (24). Similar to the non-replicative case, the optimal controls may now be obtained [via (26)] by solving the above system of differential equations.

We conclude this section by stating and proving some important properties of the adjoint functions (Lemma 3) and $\phi_i(\cdot)$ (Lemma 4 subsequently), which we use later.

First, from (24), $\psi_i(0,t) = 0$, hence (26) results in $\psi_i(u_i,t) \leq 0$. Furthermore, from the definition of τ_i, if $t \leq \tau_i$, $(h_i(u_i(t)) - \phi_i(t)u_i(t)) = 0$, and if $t > \tau_i$, $(h_i(u_i(t)) - \phi_i(t)u_i(t)) = \frac{\psi_i(u_i,t)}{R_i(t)} \leq 0$, so for all t

$$\alpha_i(u_i,t) := (h_i(u_i(t)) - \phi_i(t)u_i(t)) \leq 0. \tag{29}$$

Lemma 3: For all $t \in [0,T)$ and for all i, we have $(\lambda_i^{\mathrm{I}} - \lambda_i^{\mathrm{S}}) > 0$ and $(\lambda_i^{\mathrm{I}} - \lambda_i^{\mathrm{R}}) > 0$.

Using our previous intuitive analogy, Lemma 3 implies that infective nodes are always worse for the evolution of the system than either susceptible or healed nodes, and thus the marginal price of infectives is greater than that of susceptible and healed nodes at all times before T. As before, we defer the proof of this lemma (to Section IV-C) to avoid breaking up the flow of the narrative. We now state and prove Lemma 4.

Lemma 4: For each i, $\phi_i(t)$ is a decreasing function of t, and $\dot{\phi}_i(t^+) < 0$ and $\dot{\phi}_i(t^-) < 0$ for all t.

Proof: $\phi_i(t)$ is continuous everywhere (due to the continuity of the states and adjoint functions) and differentiable whenever $\mathbf{u}(\cdot)$ is continuous. At any t at which $\mathbf{u}(\cdot)$ is continuous, we have: $\dot{\phi}_i(t) = \sum_{j=1}^{M} \bar{\beta}_{ij}[(\dot{\lambda}_j^{\mathrm{S}} - \dot{\lambda}_j^{\mathrm{R}})S_j + (\lambda_j^{\mathrm{S}} - \lambda_j^{\mathrm{R}})\dot{S}_j + \pi_{ij}(\dot{\lambda}_j^{\mathrm{I}} - \dot{\lambda}_j^{\mathrm{R}})I_j + \pi_{ij}(\lambda_j^{\mathrm{I}} - \lambda_j^{\mathrm{R}})\dot{I}_j]$.

From (22) and the adjoint equations (23), at points of continuity of the control, we have

$$\begin{aligned}
\dot{\lambda}_i^{\mathrm{S}} &= -\left(\lambda_i^{\mathrm{I}} - \lambda_i^{\mathrm{S}}\right)\sum_{j=1}^{M}\beta_{ji}I_j - \left(\lambda_i^{\mathrm{R}} - \lambda_i^{\mathrm{S}}\right)\sum_{j=1}^{M}\bar{\beta}_{ji}R_j u_j \\
\dot{\lambda}_i^{\mathrm{I}} &= -\frac{\partial f(\mathbf{I})}{\partial I_i} - \sum_{j=1}^{M}\left(\lambda_j^{\mathrm{I}} - \lambda_j^{\mathrm{S}}\right)\beta_{ij}S_j \\
&\quad - \left(\lambda_i^{\mathrm{R}} - \lambda_i^{\mathrm{I}}\right)\sum_{j=1}^{M}\pi_{ji}\bar{\beta}_{ji}R_j u_j \\
\dot{\lambda}_i^{\mathrm{R}} &= \frac{\partial L(\mathbf{R})}{\partial R_i} + u_i\sum_{j=1}^{M}\bar{\beta}_{ij}\left(\lambda_j^{\mathrm{S}} - \lambda_j^{\mathrm{R}}\right)S_j \\
&\quad + u_i\sum_{j=1}^{M}\pi_{ij}\bar{\beta}_{ij}\left(\lambda_j^{\mathrm{I}} - \lambda_j^{\mathrm{R}}\right)I_j \\
&\quad - h_i(u_i) = \frac{\partial L(\mathbf{R})}{\partial R_i} - \alpha_i(u_i,t).
\end{aligned} \tag{30}$$

Therefore, after some regrouping and cancellation of terms, at any t, we have $-\dot{\phi}_i(t^+) = \sum_{j=1}^{M}\bar{\beta}_{ij}[(1-\pi_{ij})\sum_{k=1}^{M}(\lambda_j^{\mathrm{I}} - \lambda_j^{\mathrm{R}})\beta_{kj}I_kS_j + \pi_{ij}\frac{\partial f(\mathbf{I})}{\partial I_j}I_j + (S_j + \pi_{ij}I_j)(\frac{\partial L(\mathbf{R})}{\partial R_j} - \alpha_i(u_i,t)) + \pi_{ij}I_j\sum_{k=1}^{M}(\lambda_k^{\mathrm{I}} - \lambda_k^{\mathrm{S}})\beta_{jk}S_k]$. Now, since $0 \leq \pi_{ij} \leq 1$, the assumptions on $\bar{\beta}_{ij}, \beta_{ki}, \beta_{il}$, Theorem 1, and Lemma 3 altogether imply that the sum of the first and last terms of the RHS will be positive. The second and third terms will be nonnegative due to the definitions of $f(\cdot)$ and $L(\cdot)$ and (29). Thus, $\dot{\phi}_i(t^+) < 0$ for all t. The proof for $\dot{\phi}_i(t^-) < 0$ is exactly as above. In a very similar fashion, it can be proved that $\dot{\phi}_i(t) < 0$ at all points of continuity of $\mathbf{u}(\cdot)$, which coupled with the continuity of $\phi_i(t)$ shows that it is a decreasing function of time. □

B. Structure of Optimal Replicative Dispatch

Theorem 3: If an optimal control exists, for types i such that $R_i(t) > 0$ for some t: If $h_i(\cdot)$ is concave for type i, the optimal control for type i has the following structure: $u_i(t) = 1$ for $0 < t < t_i$, and $u_i(t) = 0$ for $t_i < t \leq T$, where $t_i \in [0,T)$. If $h_i(\cdot)$ is strictly convex, the optimal control for type i, $u_i(t)$ is continuous and has the following structure: $u_i(t) = 1$ for $0 < t < t_i^1$, $u_i(t) = 0$ for $t_i^2 < t \leq T$, and $u_i(t)$ strictly decreases in the interval $[t_i^1, t_i^2]$, where $0 \leq t_i^1 < t_i^2 \leq T$.

Notice that for i such that $R_i(t) = 0$ for all t, the control $u_i(t)$ is irrelevant and can take any arbitrary value. We first prove the theorem for $t \in [\tau_i, T]$, and then we show that $\tau_i \in \{0, T\}$, completing our proof.

Proof: First consider an i such that $h_i(\cdot)$ is concave and nonlinear. Note that hence $\psi_i(x,t)$ is a nonlinear concave function of x. Thus, the minimum can only occur at extremal values of x, i.e., $x = 0$ and $x = 1$. Now, $\psi_i(0,t) = 0$ at all times t, so to obtain the structure of the control, we need to examine $\psi_i(1,t)$ at each $t > \tau_i$. Let $\gamma_i(t) := \psi_i(1,t) = R_i(t)(h_i(1) - \phi_i(t))$ be a function of time t. From (26), the optimal u_i satisfies

$$u_i(t) = \begin{cases} 1, & \gamma_i(t) < 0 \\ 0, & \gamma_i(t) > 0. \end{cases} \tag{31}$$

We now show that $\gamma_i(t) > 0$ for an interval $(t_i, T]$ for some t_i, and $\gamma_i(t) < 0$ for $[\tau_i, t_i)$ if $t_i > \tau_i$. From (24) and (28), $\gamma_i(T) = h_i(1)R_i(T) > 0$. Since $\gamma_i(t)$ is a continuous function of its variable (due to the continuity of the states and adjoint functions), it will be positive for a nonzero interval leading up to $t = T$. If $\gamma_i(t) > 0$ for all $t \in [\tau_i, T]$, the theorem follows. Otherwise, from continuity, there must exist a $t = t_i > \tau_i$ such that $\gamma_i(t_i) = 0$. We show that for $t > t_i$, $\gamma_i(t) > 0$, from which it follows that $\gamma_i(t) < 0$ for $t < t_i$ (by a contradiction argument). The theorem will then follow from (31).

Toward establishing the above, we show that $\dot{\gamma}_i(t^+) > 0$ and $\dot{\gamma}_i(t^-) > 0$ for any t such that $\gamma_i(t) = 0$. Hence, there will exist an interval $(t_i, t_i + \epsilon)$ over which $\gamma_i(t) > 0$. If $t_i + \epsilon \geq T$, then the claim holds, otherwise there exists a $t = t_i{}' > t_i$ such that $\gamma_i(t_i{}') = 0$ and $\gamma_i(t) \neq 0$ for $t_i < t < t_i{}'$ (from the continuity of $\gamma_i(t)$). Thus, $\dot{\gamma}_i(t_i{}'^-) > 0$, which contradicts a property of real-valued functions (proved in [8]), establishing the claim.

Property 2: If $g(x)$ is a continuous and piecewise differentiable function over $[a,b]$ such that $g(a) = g(b)$ while $g(x) \neq g(a)$ for all x in (a,b), $\frac{dg}{dx}(a^+)$ and $\frac{dg}{dx}(b^-)$ cannot be positive simultaneously.

We now show that $\dot{\gamma}_i(t^+) > 0$ and $\dot{\gamma}_i(t^-) > 0$ for any $t > \tau_i$ such that $\gamma_i(t) = 0$. Due to the continuity of $\gamma_i(t)$ and the states, and the finite number of points of discontinuity of the controls, for any $t > \tau_i$ we have $\dot{\gamma}_i(t^+) = (\dot{R}_i(t^+)\frac{\gamma_i(t)}{R_i(t)} - R_i(t)\dot{\phi}_i(t^+))$ and $\dot{\gamma}_i(t^-) = (\dot{R}_i(t^-)\frac{\gamma_i(t)}{R_i(t)} - R_i(t)\dot{\phi}_i(t^-))$. If $\gamma_i(t) = 0$, then

$\dot{\gamma}_i(t^+) = -R_i(t)\dot{\phi}_i(t^+)$ and $\dot{\gamma}_i(t^-) = -R_i(t)\dot{\phi}_i(t^-)$, which are both positive from Lemma 4 and Theorem 1, and thus the theorem follows.

The proofs for linear and strictly convex $h_i(\cdot)$'s are virtually identical to the corresponding parts of the proof of Theorem 2 and are omitted for brevity; the only difference is that in the linear case we need to replace R_i^0 with $R_i(t)$. The following lemma, proved in Section IV-D, completes the proof of the theorem.

Lemma 5: For all $0 \leq i \leq B$, $\tau_i \in \{0, T\}$. ■

C. Proof of Lemma 3

Proof: First, from (28) and (24), we have $\phi_i(T) = 0$, which, combined with (27), results in $\psi_i(x, T) = R_i(T)h_i(x)$. Since either $R_i(T) > 0$ or $\tau_i > T$, (26) and the definition of u_i result in $u_i(T) = 0$, as all other values of x would produce a positive $\psi_i(x, T)$. Therefore, $h_i(u_i(T)) = 0$.

The rest of the proof has a similar structure to that of Lemma 1. $(\lambda_i^{\mathrm{I}} - \lambda_i^{\mathrm{S}})|_{t=T} = 0$ and $\lim_{t\uparrow T}(\dot{\lambda}_i^{\mathrm{I}} - \dot{\lambda}_i^{\mathrm{S}}) = -\partial f(\mathbf{I})/\partial I_i < 0$, for all i. Also, for all i, $(\lambda_i^{\mathrm{I}} - \lambda_i^{\mathrm{R}})|_{t=T} = 0$ and $\lim_{t\uparrow T}(\dot{\lambda}_i^{\mathrm{I}} - \dot{\lambda}_i^{\mathrm{R}}) = -\partial f(\mathbf{I})/\partial I_i - \partial L(\mathbf{R})/\partial R_i + h_i(u_i(T)) < 0$, since $h_i(u_i(T)) = 0$.

Hence, $\exists \epsilon > 0$ such that $(\lambda_i^{\mathrm{I}} - \lambda_i^{\mathrm{S}}) > 0$ and $(\lambda_i^{\mathrm{I}} - \lambda_i^{\mathrm{R}}) > 0$ over $(T - \epsilon', T)$.

Now suppose that (at least) one of the inequalities is first[12] violated at $t = t^*$ for i^*, i.e., for all i, $(\lambda_i^{\mathrm{I}}(t) - \lambda_i^{\mathrm{S}}(t)) > 0$ and $(\lambda_i^{\mathrm{I}}(t) - \lambda_i^{\mathrm{R}}(t)) > 0$ for all $t > t^*$, and either: A) $(\lambda_{i^*}^{\mathrm{I}}(t^*) - \lambda_{i^*}^{\mathrm{S}}(t^*)) = 0$; or B) $(\lambda_{i^*}^{\mathrm{I}}(t^*) - \lambda_{i^*}^{\mathrm{R}}(t^*)) = 0$ for some i^*. Note that from continuity of the adjoint functions, $(\lambda_i^{\mathrm{I}}(t^*) - \lambda_i^{\mathrm{S}}(t^*)) \geq 0$, and $(\lambda_i^{\mathrm{I}}(t^*) - \lambda_i^{\mathrm{R}}(t^*)) \geq 0$ for all i.

Case A: Here, we have:[13] $(\dot{\lambda}_{i^*}^{\mathrm{I}} - \dot{\lambda}_{i^*}^{\mathrm{S}})(t^{*+}) = -\frac{\partial f(\mathbf{I})}{\partial I_{i^*}} - \sum_{j=1}^{M}(\lambda_j^{\mathrm{I}} - \lambda_j^{\mathrm{S}})\beta_{i^*j}S_j - (\lambda_{i^*}^{\mathrm{I}} - \lambda_{i^*}^{\mathrm{R}})\sum_{j=1}^{M}\bar{\beta}_{ji^*}(1-\pi_{ji^*})R_j u_j$. First of all, $-\partial f(\mathbf{I})/\partial I_{i^*} < 0$. Also, the second and third terms are nonpositive, according to the definition of t^*. Hence, $(\dot{\lambda}_{i^*}^{\mathrm{I}} - \dot{\lambda}_{i^*}^{\mathrm{S}})(t^{*+}) < 0$, which contradicts Property 1, therefore Case A does not arise.

Case B: In this case, we have:[13] $(\dot{\lambda}_{i^*}^{\mathrm{I}} - \dot{\lambda}_{i^*}^{\mathrm{R}})(t^{*+}) = -\frac{\partial f(\mathbf{I})}{\partial I_{i^*}} - \frac{\partial L(\mathbf{R})}{\partial R_{i^*}} - \sum_{j=1}^{M}(\lambda_j^{\mathrm{I}} - \lambda_j^{\mathrm{S}})\beta_{i^*j}S_j + \alpha_{i^*}(u_{i^*}, t)$.

We have $-\partial f(\mathbf{I})/\partial I_{i^*} < 0$ and $-\partial L(\mathbf{R})/\partial R_{i^*} \leq 0$. The term $-(\lambda_{i^*}^{\mathrm{I}} - \lambda_{i^*}^{\mathrm{S}})\sum_{j=1}^{M}\beta_{ji^*}S_j$ is nonpositive, according to the definition of t^*, and α_{i^*} will be nonnegative due to (29). This shows $(\dot{\lambda}_{i^*}^{\mathrm{I}} - \dot{\lambda}_{i^*}^{\mathrm{R}})(t^{*+}) < 0$, contradicting Property 1, and so Case B does not arise either, completing the proof. □

D. Proof of Lemma 5

Proof: We start by creating another control $\bar{\mathbf{u}}$ from $\mathbf{u}$ such that for every i, for every $t \leq \tau_i$, $\bar{u}_i(t) := 1$, and for every $t > \tau_i$, $\bar{u}_i(t) := u_i(t)$. We prove by contradiction that $\tau_i(\mathbf{I}(0), \mathbf{S}(0), \mathbf{R}(0), \bar{\mathbf{u}}) \in \{0, T\}$ for each i. Since $\bar{u}_i \neq u_i$ only in $[0, \tau_i]$ and $R_i(t) = 0$ for $t \in (0, \tau_i]$ when $\mathbf{u}$ is used, the state equations can only differ at a solitary point $t = 0$, and therefore both controls result in the same state evolutions. Thus, for each i, $\tau_i(\mathbf{I}(0), \mathbf{S}(0), \mathbf{R}(0), \bar{\mathbf{u}}) = \tau_i(\mathbf{I}(0), \mathbf{S}(0), \mathbf{R}(0), \mathbf{u})$, and $\tau_i(\mathbf{I}(0), \mathbf{S}(0), \bar{\mathbf{u}})$ may be denoted as τ_i as well. The lemma therefore follows.

[12]Going backward in time from $t = T$.

[13]The RHS of the equation is evaluated at $t = t^*$ due to continuity.

For the contradiction argument, assume that the control is $\bar{\mathbf{u}}$ and that $\tau_i \in (0, T)$ for some i. Our proof relies on the fact that if $\bar{u}_i(t') = 0$ at some $t' \in (0, T)$, then $\bar{u}_i(t) = 0$ for $t > t'$, which follows from the definition of $\bar{\mathbf{u}}$ and prior results in the proof of Theorem 3.

For $t \in [0, \tau_i]$, since $R_i(t) = 0$ in this interval, (5c) becomes $\dot{R}_i = \sum_{j=1, j\neq i}^{M}\bar{\beta}_{ji}(S_i + \pi_{ji}I_i)R_j\bar{u}_j = 0$ in this interval. Since all terms in $\sum_{j=1,j\neq i}^{M}\bar{\beta}_{ji}(S_i + \pi_{ji}I_i)R_j\bar{u}_j$ are nonnegative, for each $j \neq i$, we must either have: i) $\bar{\beta}_{ji}(S_i(t) + \pi_{ji}I_i(t)) = 0$ for some $t \in [0, \tau_i]$; or ii) $R_j(t)\bar{u}_j(t) = 0$ for all $t \in [0, \tau_i]$.

i) Here, either $\bar{\beta}_{ji} = 0$; or $(S_i(t) + \pi_{ji}I_i(t)) = 0$, and hence due to Theorem 1, $S_i(t) = 0$ and $\pi_{ji}I_i(t) = 0$. In the latter case, from Theorem 1, $S_i(0) = 0$ and $\pi_{ji} = 0$, and therefore for all $t > 0$, we will have $\bar{\beta}_{ji}(S_i + \pi_{ji}I_i)R_j\bar{u}_j = 0$.

ii) We can assume $\bar{\beta}_{ji}(S_i(t) + \pi_{ji}I_i(t)) > 0$ for all $t \in (0, \tau_i]$. For such j, if $\tau_j < \tau_i$, $R_j(t) > 0$ for $t \in (\tau_j, \tau_i]$, therefore $\bar{u}_j(t) = 0$ for such t. Due to the structure results obtained for the interval $[\tau_j, T]$ in Theorem 3, $\bar{u}_j(t) = 0$ for all $t > \tau_j$, and therefore $\bar{\beta}_{ji}(S_i + \pi_{ji}I_i)R_j\bar{u}_j = 0$ for all $t > 0$.

Now, since $M < \infty$, the set $W = \{\tau_k : \tau_k > 0, k = 1, \ldots, M\}$ must have a minimum $\omega_0 < T$. Let $L(\omega_0) = \{k \in \{1, \ldots, M\} : \tau_k = \omega_0\}$. Let the second smallest element in W be ω_1. Using the above argument, the values of $R_k(t)$ for $t \in [\omega_0, \omega_1]$ for all $k \in L(\omega_0)$ would affect each other, but not R_i's for i such that $\tau_i > 0$, $i \notin L(\omega_0)$. Furthermore, in this interval for $k \in L(\omega_0)$, we have $\dot{R}_k = \sum_{g\in L(\omega_0)}\bar{\beta}_{gk}(S_g + \pi_{gk}I_i)R_g\bar{u}_g$, with $R_k(\omega_0) = 0$. We see that for all $k \in L(\omega_0)$, replacing $R_k(t) = 0$ in the RHS of (5) gives us $\dot{R}_k(t) = 0$, a compatible left-hand side (LHS), while not compromising the existence of solutions for all other states. An application of Theorem 1 for $t \in [\omega_0, \omega_1]$ and $\bar{u}$ shows that this is the unique solution of the system of differential equations (5). This contradicts the definition of τ_k, completing the proof of the lemma. □

V. Alternative Cost Functional

Recall that in our objective function, the cost of non-replicative patching was defined as $\sum_{i=1}^{M} R_i^0 h_i(u_i)$ (respectively, $\sum_{i=1}^{M} R_i h_i(u_i)$ for the replicative case), which corresponds to a scenario in which the dispatchers are charged for every instant they are immunizing/healing (distributing the patch), irrespective of the number of nodes to which they are delivering patches. This represents a *broadcast* cost model where each transmission can reach all nodes of the neighboring types. In an alternative *unicast* scenario, different transmissions may be required to deliver the patches to different nodes. This model is particularly useful if the dispatchers may only transmit to the nodes that have not yet received the patch.[14] Hence, the cost of patching in this case can be represented by: $\sum_{i=1}^{M}\sum_{j=1}^{M} R_i^0\bar{\beta}_{ij}(S_j + I_j)p(u_i)$ (for the replicative case:

[14]This can be achieved by keeping a common database of nodes that have successfully received the patch, or by implementing a turn-taking algorithm preventing double targeting. Note that we naturally assume that the network does not know with *a priori* certainty which nodes are infective, and hence it cannot differentiate between susceptibles and infectives. Consequently, even when $\pi_{ij} = 0$, i.e., the system manager knows the patch cannot remove the infection and can only immunize the susceptible, still the best it may be able to do is to forward the message to any node that has not yet received it.

$\sum_{i=1}^{M}\sum_{j=1}^{M} R_i\bar{\beta}_{ij}(S_j+I_j)p(u_i))$, where $p(\cdot)$ is an increasing function. More generally, the patching cost can be represented as a sum of the previously seen cost (Section II-E) and this term.

For non-replicative patching, if all $h_i(\cdot)$ and $p(\cdot)$ are concave, then Theorem 2 will hold if for all pairs (i,j), $\pi_{ij}=\pi_j$ (i.e., healing efficacy only depends on the type of an infected node, not that of the immunizer). The analysis will change in the following ways: A term of $R_i^0 p(u_i)\sum_{j=1}^{M}\bar{\beta}_{ij}(S_j+I_j)$ is added to (15), and subsequently to (18) (with $u_i=1$ in the latter case). Also, (17) is modified by the subtraction of $\sum_{j=1}^{M}\bar{\beta}_{ji}R_j^0 p(u_j)$ from the RHS of both equations. This leaves $\dot{\lambda}_i^{\mathrm{I}}-\dot{\lambda}_i^{\mathrm{S}}$ untouched, while subtracting a positive amount from $\dot{\lambda}_i^{\mathrm{I}}$, meaning that Lemma 1 still holds. As $\phi_i(t)$ was untouched, this means that Lemma 2 will also hold. Thus, the RHS of $\dot{\gamma}_i$ is only modified by the subtraction of $\sum_{j,k=1}^{M}\bar{\beta}_{ij}(S_j+\pi_j I_j)\bar{\beta}_{kj}R_k^0(p(u_k)-u_k p(1))$, which is a positive term, as for any continuous, increasing, concave function $p(\cdot)$ such that $p(0)=0$, we have $ap(b)\geq bp(a)$ if $a\geq b\geq 0$ since $\frac{p(x)}{x}$ is increasing. This yields: $(p(u_k)-u_k p(1)\geq 0)$. Therefore the conclusion of Theorem 2 holds. Similarly, it may be shown that Theorem 2 also holds for strictly convex $h_i(\cdot)$ provided $p(\cdot)$ is linear.

For the replicative case, if $p(\cdot)$ is linear $(p(x)=Cx)$ and again $\pi_{ij}=\pi_j$ for all (i,j), Theorem 3 will hold. The modifications of the integrand and ψ_i are as above. The adjoint equations (30) are modified by the subtraction of $\sum_{j=1}^{M}C\bar{\beta}_{ji}R_j u_j$ from $\dot{\lambda}_i^{\mathrm{I}}$ and $\dot{\lambda}_i^{\mathrm{I}}$, and the subtraction of $Cu_i\sum_{j=1}^{M}\bar{\beta}_{ij}(S_j+I_j)$ from $\dot{\lambda}_i^{\mathrm{R}}$. Due to the simultaneous change in ψ_i, however, we still have $\dot{\lambda}_i^{\mathrm{R}}=\partial L(\mathbf{R})/\partial R_i-\alpha_i(u_i,t)$. Therefore, Lemma 3 still holds, as $\dot{\lambda}_i^{\mathrm{I}}-\dot{\lambda}_i^{\mathrm{S}}$ is unchanged, and a positive amount is subtracted from $\dot{\lambda}_i^{\mathrm{I}}-\dot{\lambda}_i^{\mathrm{R}}$. We absorb $\sum_{j=1}^{M}C\bar{\beta}_{ij}(S_j+I_j)$ into $\phi_i(t)$, where all the $p(\cdot)$ terms in $\dot{\phi}_i$ will cancel out, leaving the rest of the analysis, including for Lemmas 4 and 5, to be the same. The theorem follows.

VI. Numerical Investigations

In this section, we numerically investigate the optimal control policies for a range of malware and network parameters and examine its performance in a real-world traces.[15] We first present an example of our optimal policy (Section VI-1), and then we examine its behavior in some sample topologies (Section VI-2). Subsequently, we present four heuristics that are likely to arise in practice and show the cost improvements the optimal policy is likely to show (Section VI-3) and demonstrate the relative benefits of replicative, as opposed to non-replicative, patching (Section VI-4). For an emerging epidemic, the initial conditions and the contact rates β_{ij} may not immediately be known. However, these parameters can be estimated by the network by looking at the empiric contact frequencies of a small number of nodes. Furthermore, nodes may have synchronization issues that affect the implementation of a time-sensitive policy. In Section VI-5, we investigate the optimal policy's robustness to errors in estimation of the initial states, mixing rates, and in the synchronization of the node clocks. Finally, in Section VI-6, we examine how our optimal policy performs on a real trace of mobility and communication.

[15]For our calculations, we used *C* and *MATLAB* programming.

TABLE I
Simulation Parameters: Here, Rep Shows Whether the Patching Is Replicative, X_C Is X_{Coef}, and C Is Cost Type. In All Cases, $K_I=1$. Dashed Parameters Are Simulation Variables

Fig.	Top.	Rep	π	M	T	C	X_C	$\mathbf{R}^0$	$\mathbf{I}^0$	K_U
2	Lin.	N	-	3	35	A	0.1	$\{0.2\}_1^M$	$0.3,\{0\}_2^M$	0.5
3	Lin.	N	-	10	35	A	-	$\{0.2\}_1^M$	$0.3,\{0\}_2^M$	0.5
4	Star	N	-	-	35	B	0.1	$\{0.2\}_1^M$	$0.6,\{0\}_2^M$	0.2
5	Lin.	Y	1	-	35	A	0.1	$\{0.2\}_1^M$	$0.2,\{0\}_2^M$	0.2
6	Comp.	Y	1	-	35	A	0.1	$\{0.2\}_1^M$	$0.3,\{0\}_2^M$	0.2
7A	Ring	N	1	4	10	A	0.2	$0.05,\{0.01\}_2^M$	$0.1,\{0\}_2^M$	0.01
7B	Ring	N	0	4	35	A	0.1	$\{0.1\}_1^M$	$0.4,\{0\}_2^M$	0.07
7C	Ring	N	1	4	20	A	0.5	$\{0.01\}_1^M$	$0.05,\{0\}_2^M$	0.01

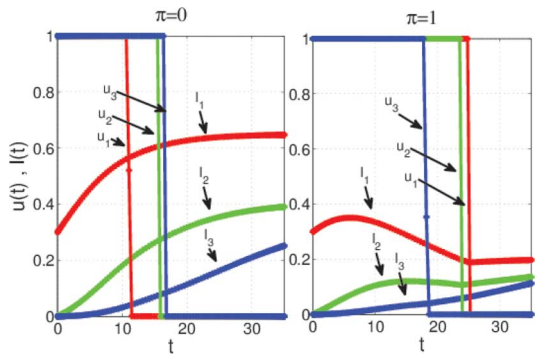

Fig. 2. Optimal patching policies and corresponding levels of infection in a 3-region linear topology. Note how the infection that initially only exists in region 1 spreads in region 1 and then to region 2, and finally to region 3.

Recalling the notion of topologies presented in Section II-A [in the paragraph before (2)], we consider *four* topologies: *linear*, *ring*, *star* and *complete*, as was illustrated in Fig. 1. We assume $\beta_{ii}=\beta=0.223$ for all i.[16] The value of β_{ij}, $i\neq j$ is equal to $X_{\mathrm{Coef}}\cdot\beta$ if link ij is part of the topology graph, and zero otherwise. It should be noted that $\beta_{ij}*T$ denotes the average number of contacts between nodes of regions i and j within the time period, and thus β and T are dependent variables. For simplicity, we use equal values for $\beta_{ji},\beta_{ij},\bar{\beta}_{ij},\bar{\beta}_{ji}$ for all i,j (i.e., $\beta_{ji}=\beta_{ij}=\bar{\beta}_{ij}=\bar{\beta}_{ji}$), and set $\pi_{ij}=\pi$ for all i,j. We examine two different aggregate cost structures for non-replicative patching:[17] (type-A)—$\int_0^T(K_I\sum_{i=1}^{M}I_i(t)+K_u\sum_{i=1}^{M}R_i^0u_i(t))\,dt$; and (type-B)—$\int_0^T(K_I\sum_{i=1}^{M}I_i(t)+K_u\sum_{i=1}^{M}R_i^0u_i(t)(S_i(t)+I_i(t)))\,dt$ (described in Sections II-E and V, respectively). For replicative patching, R_i^0 in both cost types is replaced with $R_i(t)$. The parameters for all simulations are summarized in Table I.

1) Numeric Example: First, in Fig. 2, we have depicted an example of the optimal dynamic patching policy along with the corresponding evolution of the infection as a function of time for a simple 3-region linear topology. For $\pi=0$, the levels of infection are nondecreasing, whereas for $\pi=1$, they may go down as well as up (due to healing).

2) Effects of Topology: We study the *drop-off* times (the time thresholds at which the bang-bang optimal patching halts) in different regions for linear and star topologies.

[16]This specific value of β is chosen to match the average intermeeting times from the numerical experiment reported in [41].

[17]$f_i(\cdot)$, $h_i(\cdot)$, and $p(\cdot)$ are linear and identical for all i, and $l_i(\cdot)=0$.

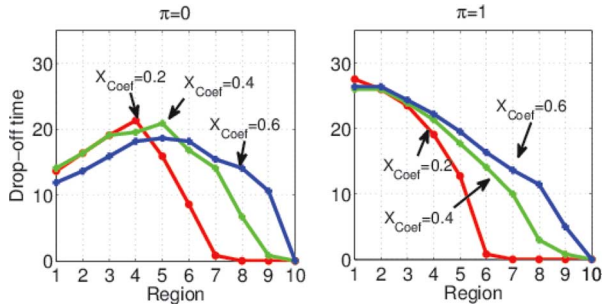

Fig. 3. Drop-off times in a linear topology for $X_{\text{Coef}} = 0.2, 0.4, 0.6$.

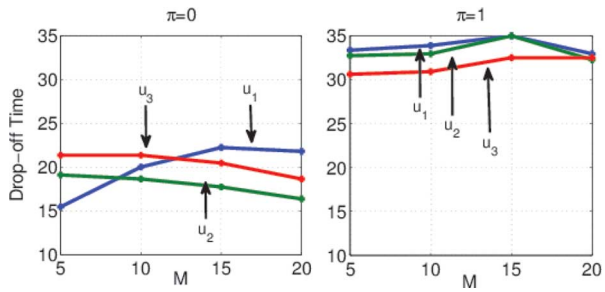

Fig. 4. Drop-off times in the star topology.

Fig. 3 reveals two different patterns for $\pi = 0$ and $\pi = 1$ in a linear topology. For $\pi = 0$, a middle region is patched for the longest time, whereas for $\pi = 1$, as we move away from the origin of the infection (region 1), the drop-off point decreases. This is because for $\pi = 0$, patching can only benefit the network by recovering susceptibles. In regions closer to the origin, the fraction of susceptibles decreases quickly, making continuation of the patching comparatively less beneficial. In the middle regions, where there are more salvageable susceptibles, patching should be continued for longer. For regions far from the origin, patching can be stopped earlier, as the infection barely reaches them within the time horizon of consideration. For $\pi = 1$, patching is able to recover both susceptible and infective nodes. Hence, the drop-off times depend only on the exposure to the infection, which decreases with distance from the origin. As X_{Coef} is increased, the drop-off points when $\pi = 1$ get closer together. Intuitively, this is because higher cross-mixing rates have a homogenizing effect, as the levels of susceptible and infective nodes in different regions rapidly become comparable. Also, Fig. 3 reveals that as X_{Coef} increases and more infection reaches farther regions, they are patched for longer, which agrees with our intuition.

We next investigate a star configuration where the infection starts from a peripheral region (region 1 in the star in Fig. 1). Fig. 4 reveals the following interesting phenomenon: Although the central region is the only one that is connected to all the regions, for $\pi = 0$, it is patched for shorter lengths of time compared to the peripherals. In retrospect, this is because only susceptible nodes can be patched and their number at the central region drops quickly due to its interactions with all the peripheral regions, rendering patching inefficient relatively swiftly. As expected, this effect is amplified with higher numbers of peripheral regions. For $\pi = 1$, on the other hand, the central region is patched for the longest time. This is because the infective nodes there can infect susceptible nodes in all regions, and hence the patching, which can now heal the infectives as well, does not stop until it heals almost all of infective nodes in this region.

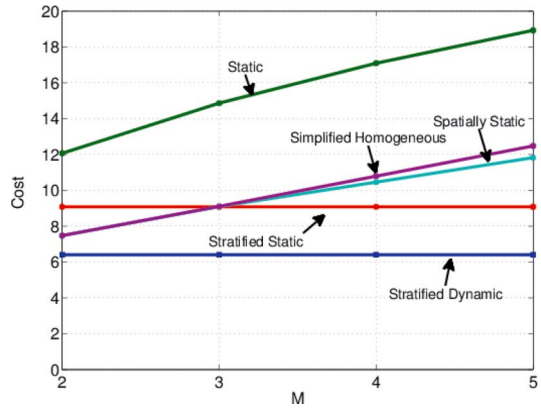

Fig. 5. Cost of heuristics versus the optimal policy, linear topology.

3) Cost Comparison: Next, in order to evaluate the efficacy of our optimal dynamic heterogeneous patching, which we henceforth refer to as *Stratified Dynamic* (S.D.), we compare our aggregate cost against those of four alternative policies.

In the simplest alternative policy, all regions use identical patching intensities that do not change with time. We then select this fixed and static level of patching so as to minimize the aggregate cost among all possible choices. We refer to this policy as *Static* (St.). The aggregate cost may be reduced if the static level of the patching is allowed to be distinct for different regions. These values (still fixed over time) are then independently varied, and the optimum combination is selected. We refer to this policy as *Stratified Static* (S. St.). The third policy we implement is a *homogeneous* approximation to the heterogeneous network. Specifically, the whole network is approximated by a single region model with an intercontact rate equal to the *mean* pairwise contact rate of the real system. The optimal control is derived based on this model and applied across all regions to calculate the aggregate cost. We call this policy *Simplified Homogeneous* (S. H.). The simplified homogeneous policy is a special case of Spatially Static (Sp. St.) policies: Sp. St. policies optimize a *single* jump point for a bang-bang control to be applied to *all* types in the topology.

Fig. 5 depicts the aggregate costs of all five policies for a linear topology and intratype β_{ii} and intertype contact rates β_{ij} constant. As we can clearly observe, our stratified policy achieves the least cost, outperforming the rest. For example, for $M \geq 3$ regions, our policy outperforms the best static policies by 40%, and for $M = 5$, it betters the homogeneous approximation by 100%, which shows that our results about the structure of the optimal control can result in large cost improvements. When the number of regions is small, S. H. and Sp. St. perform better than S. St., all of which obviously outperform St. However, as the number of regions increases and the network becomes more spatially heterogeneous, the homogeneous approximation, and all uniform controls in general, worsen, and the S. St. policy quickly overtakes them as the best approximation to the optimal. In this case, the cost of the two stratified policies does not change noticeably as the number of types is increased. While this is an attribute of the simulation settings (and in particular, the linear topology), in general, S.D. and S. St. are the only two policies that can optimize controls in direct accordance with the topology. Therefore, the extent of their cost variations is less as the number of types is varied compared to the other heuristics.

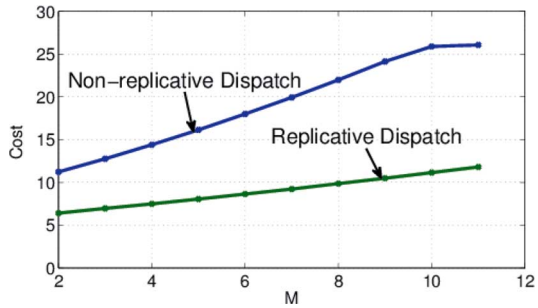

Fig. 6. Replicative and non-replicative patch cost, complete topology.

In the particular case of Fig. 5, the fraction of recovered in each type increases much faster due to the increased number of interactions, and thus less patching needs to be carried out in that type (less intensity for the stratified static case, and for a shorter period in the stratified dynamic policy). However, these effects are countered by the rising number of elements in the cost function, leading to a seemingly constant cost. For $\pi = 0$, a similar performance gap is observed. Specifically, as discussed, optimal drop-off times for this problem should vary based on the distance from the originating region, a factor that the Sp. St., S. H., and St. policies ignore.

We now present some general observations for which we do not present figures due to space constraints. From our observations, the relative performance of the optimal becomes better as the heterogeneity among the nodes increases, both in terms of topology and in terms of states. Fig. 3 is typical for the intermediate parameter range where the optimal stratified dynamic policy is not on or off all the time. For example, the optimal performs better (relative to the heuristics) in a linear topology as opposed to a complete topology (which has identical contact rates among all pairs of types). Furthermore, for example, if the initial fraction of infectives is high in all types and we have no healing ($\pi = 0$), or the time period is too short relative to the contact rates, the patch cannot spread much beyond its original nodes, and thus all policies perform at around the same level. Finally, if the cost of infection is very high or very low relative to immunization, the optimal stratified dynamic policy will be one (respectively, zero) at all times, a control that can be replicated by the constrained heuristics, and thus the gains in performance are muted.

4) Replicative Versus Non-Replicative Patching: We already know that optimal replicative patching will outperform optimal non-replicative patching. We examine the extent of the difference through numerical computation. In Fig. 6, we see the aggregate cost of optimal replicative and non-replicative patching in a complete topology as a function of the size of the network for $M \leq 11$. Here, even for such modest sizes, replicative patching can be 60% more efficient than non-replicative patching, a significant improvement. This is especially true for the complete topology and other edge-dense topologies, as in replicative patching, the patch can spread in ways akin to the malware.

5) Robustness: In this section, we simulated the robustness of our optimal control to errors in the determination of the initial states [Fig. 7(a)], the contact rates [Fig. 7(b)], and the synchronization of the node clocks [Fig. 7(c)]. In Fig. 7(a), the system estimates the number of susceptibles and infectives of an emerging epidemic in a ring topology of size $M = 3$ with an unbiased, uniformly distributed error. It then uses this estimated network to calculate optimal controls that it applies in the real settings. It can be seen that a maximum estimation error of 15% leads to a mean cost deficiency of only 5%. This performance was replicated across differing network sizes and values of the initial parameters. In Fig. 7(b), the system estimates the mean contact rates of an emerging epidemic in a ring topology of size $M = 4$ with an unbiased, uniformly distributed error. It then uses this estimated topology to calculate optimal controls that it applies in the real settings. It can be seen that an unbiased maximum estimation error of 25% changes the mean costs by less than 1%. This remarkable robustness was seen with a range of sizes and initial parameters. In Fig. 7(c), it was assumed that the optimal controls for a ring topology of size $M = 4$ had been calculated and passed on to nodes whose clocks have unbiased, uniformly distributed shifts from the reference, who then implement the bang-bang policy. Here, we plot the mean cost difference as a function of the ratio of the maximum magnitude of the synchronization error to the resolution at which the drop-off times of the optimal control were calculated, and observe that the cost barely changes even when this ratio approaches one (and the synchronization error is of the magnitude of the decision instants).

From these results, it can be seen that the optimal control is very robust to errors in these parameters, and thus can be implementable in networks where these parameters are initially unknown and have to be estimated. We have, in each case, compared the performance of the optimal control to the heuristic that is most robust to those specific types of errors—the Simplified Homogeneous (Sp. St.) approximation for errors in the determination of the initial states and the contact rates (errors in which will get averaged out among the types), and the S. St. heuristic for clock synchronization errors, as this heuristic does not depend on the clocks of the nodes and is inherently robust to such errors.

6) Real-World Trace: In this section, we calculated the optimal control (and the relevant heuristics) for a network topology derived from a real-world trace: Bluetooth data from volunteers at the SIGCOMM 2009 conference [42]. We calculated the optimal control and the heuristics for a topology with constant contact rates derived from the trace, and with one randomly chosen infective and one recovered person per each type. We applied the controls to the real proximity data of the participants over 50 runs to find the cost differential and the variance (Table II).

The SigComm09 data set includes "Bluetooth encounters, opportunistic messaging, and social profiles of 76 users of MobiClique application at SIGCOMM 2009." The participants from each country constitute a "type" for categorization. We chose five types, as there were five nationalities with more than two participants, and calculated their per-day contact rate. Patching was replicative with $\pi = 1$, $K_I = 1$, and $K_U = 0.05$. Note that in this instance, the stratified dynamic policy still outperforms all other heuristics by 15%. It is interesting to note that even the Sp. St. policy significantly outperforms the homogeneous approximation S. H., which underscores the benefits of considering node heterogeneity.

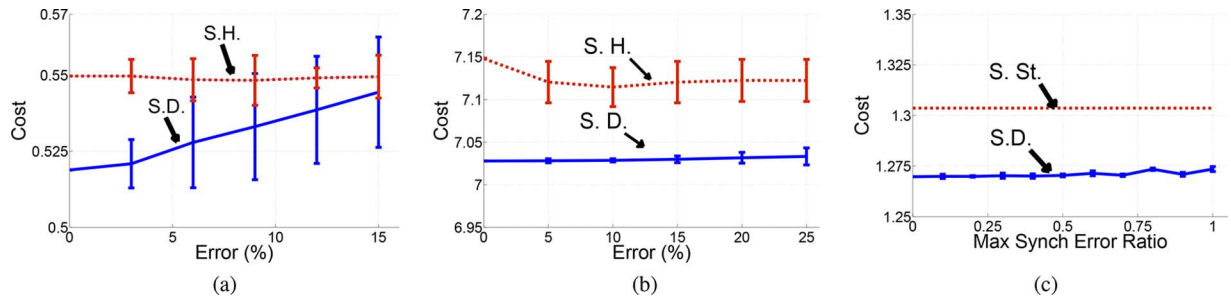

Fig. 7. Effect of errors in (a) initial condition estimation, (b) contact rate estimation, and (c) node synchronization on the mean cost of the optimal dynamic policy and the most robust heuristic. An error % of γ for the contact rate β, for example, means that the estimate is uniformly distributed in $[(1-\gamma)\beta, (1+\gamma)\beta]$. Error bars represent the cost variance over 25 runs.

TABLE II
MEAN AND VARIANCE OF THE COST OF THE POLICIES ON THE SIGCOMM09 TRACE OVER 50 RUNS

SIGCOMM09	MEAN	VARIANCE
S.D.	0.4052	0.1090
S. H.	0.6914	0.2711
S. ST.	0.8829	0.0204
SP. ST.	0.4609	0.0781
ST.	1.1667	0.0285

VII. CONCLUSION AND FUTURE WORK

We presented a general model for patch dissemination in a large heterogeneous network in the mean-field regime that can capture the core of many different types of real-world networks. We proved that optimal controls for each type have a simple structure that can be easily computed, stored, and executed in many cases of practical importance. The derived optimal controls are observed to be robust to errors in model parameter estimation and perform better than heuristics derived from practice on simulations and traces. In the future, we would like to further investigate the effects of structural heterogeneities of networks on defense and attack strategies.

APPENDIX
PROOF OF THEOREM 1

We use the following general result.

Lemma 6: Suppose the vector-valued function $\mathbf{f} = (f_i, 1 \leq i \leq 3M)$ has component functions given by quadratic forms $f_i(t, \mathbf{x}) = \mathbf{x}^T Q_i(t)\mathbf{x} + {p_i}^T\mathbf{x}$ $(t \in [0,T]; \mathbf{x} \in \mathbb{S})$, where $\mathbb{S}$ is the set of $3M$-dimensional vectors $\mathbf{x} = (x_1, \ldots, x_{3M})$ satisfying $\mathbf{x} \geq \mathbf{0}$ and $\forall j \in \{1, \ldots, M\}; x_j + x_{M+j} + x_{2M+j} = 1$, $Q_i(t)$ is a matrix whose components are uniformly, absolutely bounded over $[0,T]$, as are the elements of the vector p_i. Then, for an $3M$-dimensional vector-valued function $\mathbf{F}$, the system of differential equations

$$\dot{\mathbf{F}} = \mathbf{f}(t, \mathbf{F}) \qquad (0 < t \leq T)$$
$$\text{subject to initial conditions } \mathbf{F}(0) \in \mathbb{S} \tag{32}$$

has a unique solution, $\mathbf{F}(t)$, which varies continuously with the initial conditions $\mathbf{F}_0 \in \mathbb{S}$ at each $t \in [0,T]$.

This follows from a standard result in the theory of ordinary differential equations [43, p. 419, Theorem A.8] given that $\mathbf{f}(t, \mathbf{F})$ is comprised of quadratic and linear forms and is thus Lipschitz over $[0,T] * \mathbb{S}$.

Proof of Theorem 1: We write $\mathbf{F}(0) = \mathbf{F}_0$, and in a slightly informal notation, $\mathbf{F} = \mathbf{F}(t) = \mathbf{F}(t, \mathbf{F}_0)$ to acknowledge the dependence of $\mathbf{F}$ on the initial value $\mathbf{F}_0$.

We first verify that $\mathbf{S}(t) + \mathbf{I}(t) + \mathbf{R}(t) = \mathbf{1}$ for all t in both cases. By summing the left and right sides of the system of equations (2) and the $\dot{R}_i$ equation that was left out [respectively the two sides of equations (5)], we see that in both cases for all i, $(\dot{S}_i(t) + \dot{I}_i(t) + \dot{R}_i(t)) = 0$, and, in view of the initial normalization $(S_i(0) + I_i(0) + R_i(0)) = 1$, we have $(S_i(t) + I_i(t) + R_i(t)) = 1$ for all t and all i.

We now verify the nonnegativity condition. Let $\mathbf{F} = (F_1, \ldots, F_{3M})$ be the state vector in $3M$ dimensions whose elements comprise $(S_i, 1 \leq i \leq M)$, $(I_i, 1 \leq i \leq M)$, and $(R_i, 1 \leq i \leq M)$ in some order. The system of equations (2) can thus be represented as $\dot{\mathbf{F}} = \mathbf{f}(t, \mathbf{F})$, where for $t \in [0,T]$ and $\mathbf{x} \in \mathbb{S}$, the vector-valued function $\mathbf{f} = (f_i, 1 \leq i \leq 3M)$ has component functions $f_i(t, \mathbf{x}) = \mathbf{x}^T Q_i(t)\mathbf{x} + {p_i}^T\mathbf{x}$ in which: 1) $Q_i(t)$ is a matrix whose nonzero elements are of the form $\pm\beta_{jk}$; 2) the elements of $p_i(t)$ are of the form $\pm\bar{\beta}_{jk}R_j^0 u_j$ and $\pm\bar{\beta}_{jk}\pi_{jk}R_j^0 u_j$, whereas (5) can be represented in the same form but with: 1) $Q_i(t)$ having elements $\pm\beta_{jk}$, $\pm\bar{\beta}_{jk}u_j$, and $\pm\bar{\beta}_{jk}\pi_{jk}u_j$; and 2) $p_i = \mathbf{0}$. Thus, the components of $Q_i(t)$ are uniformly, absolutely bounded over $[0,T]$. Lemma 6 establishes that the solution $\mathbf{F}(t, \mathbf{F}_0)$ to the systems (2) and (5) is unique and varies continuously with the initial conditions $\mathbf{F}_0$; it clearly varies continuously with time. Next, using elementary calculus, we show in the next paragraph that if $\mathbf{F}_0 \in \mathbf{Int}\ \mathbb{S}$ (and, in particular, each component of $\mathbf{F}_0$ is positive), then each component of the solution $\mathbf{F}(t, \mathbf{F}_0)$ of (2) and (5) is positive at each $t \in [0,T]$. Since $\mathbf{F}(t, \mathbf{F}_0)$ varies continuously with $\mathbf{F}_0$, therefore $\mathbf{F}(t, \mathbf{F}_0) \geq \mathbf{0}$ for all $t \in [0,T]$, $\mathbf{F}_0 \in \mathbb{S}$, which completes the overall proof.

Accordingly, let the S_i, I_i, and R_i component of $\mathbf{F}_0$ be positive. Since the solution $\mathbf{F}(t, \mathbf{F}_0)$ varies continuously with time, there exists a time, say $t' > 0$, such that each component of $\mathbf{F}(t, \mathbf{F}_0)$ is positive in the interval $[0, t')$. The result follows trivially if $t' \geq T$. Suppose now that there exists $t'' < T$ such that each component of $\mathbf{F}(t, \mathbf{F}_0)$ is positive in the interval $[0, t'')$, and at least one such component is 0 at t''.

We first examine the non-replicative case. We show that such components cannot be S_i for any i and subsequently rule out I_i and R_i for all i. Note that $u_j(t), I_j(t), S_j(t)$ are bounded in $[0, t'']$ (recall $(S_j(t) + I_j(t) + R_j(t)) = 1, S_j(t) \geq 0, I_j(t) \geq 0, R_j(t) \geq 0$ for all $j \in \{1, \ldots, M\}, t \in [0, t'']$). From (2a), $S_i(t'') = S_i(0)e^{-\int_0^{t''} \sum_{j=1}^{M} (\beta_{ji} I_j(t) + \bar{\beta}_{ji} R_j^0 u_j(t))\, dt}$.

Since all $u_j(t), I_j(t)$ are bounded in $[0, t'']$, $S_i(0) > 0, R_j^0 \geq 0$, and $\beta_{ji}, \bar{\beta}_{ji} \geq 0$, therefore $S_i(t'') > 0$. Since $S_i(t) > 0$, $I_i(t) \geq 0$ for all $i, t \in [0, t'']$, and $\beta_{ji} \geq 0$, from (2b), $\dot{I}_i \geq -I_i \sum_{j=1}^{M} \pi_{ji} \bar{\beta}_{ji} R_j^0 u_j$ for all i in the interval $[0, t'']$. Thus, $I_i(t'') \geq I_i(0) e^{-\int_0^{t''} \sum_{j=1}^{M} \pi_{ji} (\bar{\beta}_{ji} R_j^0 u_j(t))\, dt}$. Since all $u_j(t), I_j(t), S_j(t)$ are bounded in $[0, t'']$, and $I_i(0) > 0$, $\bar{\beta}_{ji}, \pi_{ji} \geq 0$, it follows that $I_i(t'') > 0$ for all $i \geq 0$. Finally, $R_i(t'') > 0$ because $R_i(0) > 0$ and $\dot{R}_i(t) \geq 0$ from the above, so $R_i(t) \geq R_i^0$, and $S_i(t) + I_i(t) \leq 1 - R_i^0$ for all t and i. This contradicts the definition of t'' and in turn implies that $\mathbf{F}(t, \mathbf{F}_0) > 0$ for all $t \in [0, T]$, $\mathbf{F}_0 \in \mathbf{Int}\ \mathbb{S}$.

The proof for the replicative case is similar, with the difference that R_i^0 is replaced with R_i, which is itself bounded.

Since the control and the unique state solution $\mathbf{S}(t), \mathbf{I}(t)$ are nonnegative, (2a) and (5a) imply that $\mathbf{S}(t)$ is a nonincreasing function of time. Thus, $S_j(t) = 0$ if $S_j(0) = 0$ for any j. Using the argument in the above paragraph and starting from a $t' \in [0, T)$ where $S_j(t') > 0$, $I_j(t') > 0$, or $R_j(t') > 0$, it may be shown respectively that $S_j(t) > 0, I_j(t) > 0$, and $R_j(t) > 0$ for all $t > t'$. All that remains to show now is Lemma 7.

Lemma 7: There exists $\epsilon > 0$ such that $\mathbf{I}(t) > 0$ for $t \in (0, \epsilon)$.

Let $d(i, j)$ be the *distance* from type j to type i (i.e., for all i, $d(i, i) = 0$ and for all pairs (i, j), $d(i, j) = 1+$ minimum number of types in a path from type j to type i). Now, define $d(i, U) := \min_{j \in U} d(i, j)$, where $U := \{ i : I_i^0 > 0 \}$. Since we assumed that every type i is either in U or is connected to a type in U, $d(i, U) < M$ for all types i.

Let $\delta > 0$ be a time such that for all types i such that $d(i, U) = 0$ (the initially infected types), we have $I_i(t) > 0$ for $t \in [0, \delta)$. Thus, proving Lemma 8 will be equivalent to proving Lemma 7, given an appropriate scaling of δ.

Lemma 8: For all i and for all integers $r \geq 0$, if $d(i, U) \leq r$, then $I_i(t) > 0$ for $t \in (\frac{r}{M}\delta, T)$.

Proof: By induction on r.

Base Case: $r = 0$. If $d(i, U) = 0$, this means that the type is initially infected, and thus $I_i(t) > 0$ for $t \in (0, T)$ by definition. Therefore, the base case holds.

Induction Step: Assume that the statement holds for $r = 0, \ldots, k$ and consider $r = k + 1$. Since $(\frac{k+1}{M}\delta, T) \subset (\frac{k}{M}\delta, T)$, we need to examine types i such that $d(i, U) = k + 1$. In (2b) at $t = \frac{k+1}{M}\delta$, the first sum on the right involves terms like $I_j(\frac{k+1}{M}\delta) S_i(\frac{k+1}{M}\delta)$ where j is a neighbor of i, while the second sum involves terms like $I_i(\frac{k+1}{M}\delta) u_j(\frac{k+1}{M}\delta)$. Since $d(i, U) = k + 1$, there exist neighbors j of i such that $d(j, U) = k$, and therefore $I_j(t) > 0$ for $t \in [\frac{k+1}{M}\delta, T)$ (by the induction hypothesis). Hence, since $S_i^0 > 0$ and $\beta_{ji} > 0$ (i and j being neighbors), for such t, $\dot{I}_i(t) > -I_i(t) \sum_{j=1}^{M} \pi_{ji} \bar{\beta}_{ji} R_j^0 u_j(t) \geq -G I_i(t)$, where $G \geq 0$ is an upper bound on the sum (continuous functions are bounded on a closed and bounded interval). Thus, $I_i(t) > I_i(\frac{k+1}{M}\delta) e^{-Kt} > 0$, completing the proof for $r = k + 1$. ■

REFERENCES

[1] K. Ramachandran and B. Sikdar, "On the stability of the malware free equilibrium in cell phones networks with spatial dynamics," in *Proc. IEEE ICC*, 2007, pp. 6169–6174.

[2] P. Wang, M. C. González, C. A. Hidalgo, and A.-L. Barabási, "Understanding the spreading patterns of mobile phone viruses," *Science*, vol. 324, no. 5930, pp. 1071–1076, 2009.

[3] Z. Zhu, G. Cao, S. Zhu, S. Ranjan, and A. Nucci, "A social network based patching scheme for worm containment in cellular networks," in *Proc. IEEE INFOCOM*, 2009, pp. 1476–1484.

[4] H. Leyden, "Blaster variant offers fix for pox-ridden PCs," *Register* 2003 [Online]. Available: http://www.theregister.co.uk/2003/08/19/blaster_variant_offers_fix/

[5] W. H. Murray, "The application of epidemiology to computer viruses," *Comput. Security*, vol. 7, no. 2, pp. 139–145, 1988.

[6] J. O. Kephart and S. R. White, "Directed-graph epidemiological models of computer viruses," in *Proc. IEEE Comput. Soc. Symp. Res. Security Privacy*, 1991, pp. 343–359.

[7] Y. Li, Z. Wang, D. Jin, L. Zeng, and S. Chen, "Collaborative vehicular content dissemination with directional antennas," *IEEE Trans. Wireless Commun.*, vol. 11, no. 4, pp. 1301–1306, Apr. 2012.

[8] M. Khouzani, S. Sarkar, and E. Altman, "Maximum damage malware attack in mobile wireless networks," *IEEE/ACM Trans. Netw.*, vol. 20, no. 5, pp. 1347–1360, Oct. 2012.

[9] E. Altman, A. P. Azad, T. Basar, and F. De Pellegrini, "Optimal activation and transmission control in delay tolerant networks," in *Proc. IEEE INFOCOM*, 2010, pp. 1–5.

[10] M. Khouzani, S. Sarkar, and E. Altman, "Dispatch then stop: Optimal dissemination of security patches in mobile wireless networks," in *Proc. IEEE CDC*, 2010, pp. 2354–2359.

[11] M. Khouzani, S. Sarkar, and E. Altman, "Optimal control of epidemic evolution," in *Proc. IEEE INFOCOM*, 2011, pp. 1683–1691.

[12] Y. Li *et al.*, "Energy-efficient optimal opportunistic forwarding for delay-tolerant networks," *IEEE Trans. Veh. Technol.*, vol. 59, no. 9, pp. 4500–4512, Nov. 2010.

[13] E. Altman, G. Neglia, F. De Pellegrini, and D. Miorandi, "Decentralized stochastic control of delay tolerant networks," in *Proc. IEEE INFOCOM*, 2009, pp. 1134–1142.

[14] J. Mickens and B. Noble, "Modeling epidemic spreading in mobile environments," in *Proc. 4th ACM Workshop Wireless Security*, 2005, pp. 77–86.

[15] K. Ramachandran and B. Sikdar, "Modeling malware propagation in networks of smart cell phones with spatial dynamics," in *Proc. IEEE INFOCOM*, 2007, pp. 2516–2520.

[16] Z. Chen and C. Ji, "Spatial-temporal modeling of malware propagation in networks," *IEEE Trans. Neural Netw.*, vol. 16, no. 5, pp. 1291–1303, Sep. 2005.

[17] F. Li, Y. Yang, and J. Wu, "CPMC: An efficient proximity malware coping scheme in smartphone-based mobile networks," in *Proc. IEEE INFOCOM*, 2010, pp. 1–9.

[18] Y. Yang, S. Zhu, and G. Cao, "Improving sensor network immunity under worm attacks: A software diversity approach," in *Proc. 9th ACM Int. Symp. Mobile Ad Hoc Netw. Comput.*, 2008, pp. 149–158.

[19] Y. Li, P. Hui, L. Su, D. Jin, and L. Zeng, "An optimal distributed malware defense system for mobile networks with heterogeneous devices," in *Proc. IEEE SECON*, 2011, pp. 1–9.

[20] H. Nguyen and Y. Shinoda, "A macro view of viral propagation and its persistence in heterogeneous wireless networks," in *Proc. 5th IEEE Int. Conf. Netw. Services*, 2009, pp. 359–365.

[21] M. Liljenstam, Y. Yuan, B. Premore, and D. Nicol, "A mixed abstraction level simulation model of large-scale internet worm infestations," in *Proc. 10th IEEE MASCOTS*, 2002, pp. 109–116.

[22] M. Faghani and H. Saidi, "Malware propagation in online social networks," in *Proc. 4th IEEE MALWARE*, 2009, pp. 8–14.

[23] G. Zyba, G. Voelker, M. Liljenstam, A. Méhes, and P. Johansson, "Defending mobile phones from proximity malware," in *Proc. IEEE INFOCOM*, 2009, pp. 1503–1511.

[24] M. Altunay, S. Leyffer, J. Linderoth, and Z. Xie, "Optimal response to attacks on the open science grid," *Comput. Netw.*, vol. 55, no. 1, pp. 61–73, 2010.

[25] G. Feichtinger, R. F. Hartl, and S. P. Sethi, "Dynamic optimal control models in advertising: Recent developments," *Manage. Sci.*, vol. 40, no. 2, pp. 195–226, 1994.

[26] S. P. Sethi, "Dynamic optimal control models in advertising: A survey," *SIAM Rev.*, vol. 19, no. 4, pp. 685–725, 1977.

[27] S. P. Sethi and G. L. Thompson, *Optimal Control Theory: Applications to Management Science and Economics*. Boston, MA, USA: Kluwer, 2000, vol. 101.

[28] H. Behncke, "Optimal control of deterministic epidemics," *Optimal Control Appl. Methods*, vol. 21, no. 6, pp. 269–285, 2000.

[29] K. Wickwire, "Mathematical models for the control of pests and infectious diseases: A survey," *Theoret. Population Biol.*, vol. 11, no. 2, pp. 182–238, 1977.
[30] J. Cuzick and R. Edwards, "Spatial clustering for inhomogeneous populations," *J. Royal Statist. Soc., Ser. B, Methodological*, vol. 52, no. 1, pp. 73–104, 1990.
[31] W. Hsu and A. Helmy, "Capturing user friendship in WLAN traces," presented at the IEEE INFOCOM, 2006, poster.
[32] T. Antunović, Y. Dekel, E. Mossel, and Y. Peres, "Competing first passage percolation on random regular graphs," ArXiv e-prints, 2011.
[33] Y. Li, P. Hui, D. Jin, L. Su, and L. Zeng, "Optimal distributed malware defense in mobile networks with heterogeneous devices," *IEEE Trans. Mobile Comput.*, vol. 13, no. 2, pp. 377–391, Feb. 2014.
[34] M. Khouzani, S. Eshghi, S. Sarkar, N. B. Shroff, and S. S. Venkatesh, "Optimal energy-aware epidemic routing in DTNs," in *Proc. 13th ACM Int. Symp. Mobile Ad Hoc Netw. Comput.*, 2012, pp. 175–182.
[35] T. Kurtz, "Solutions of ordinary differential equations as limits of pure jump Markov processes," *J. Appl. Probab.*, vol. 7, pp. 49–58, 1970.
[36] N. Gast, B. Gaujal, and J. Le Boudec, "Mean field for Markov decision processes: From discrete to continuous optimization," Arxiv preprint arXiv:1004.2342, 2010.
[37] B. Bollobás, *Modern Graph Theory*. New York, NY, USA: Springer-Verlag, 1998, vol. 184.
[38] R. E. Rowthorn, R. Laxminarayan, and C. A. Gilligan, "Optimal control of epidemics in metapopulations," *J. Royal Soc. Interface*, vol. 6, no. 41, pp. 1135–1144, 2009.
[39] S. P. Sethi and P. W. Staats, "Optimal control of some simple deterministic epidemic models," *J. Oper. Res. Soc.*, vol. 29, no. 2, pp. 129–136, 1978.
[40] R. F. Stengel, *Optimal Control and Estimation*. New York, NY, USA: Dover, 1994.
[41] P. Hui *et al.*, "Pocket switched networks and human mobility in conference environments," in *Proc. ACM SIGCOMM Workshop Delay-Tolerant Netw.*, 2005, p. 251.
[42] A.-K. Pietilainen, "CRAWDAD data set thlab/sigcomm2009 (v. 2012-07-15)," Jul. 2012 [Online]. Available: http://crawdad.org/thlab/sigcomm2009/
[43] A. Seierstad and K. Sydsaeter, *Optimal Control Theory With Economic Applications*. Amsterdam, The Netherlands: North-Holland, 1987, vol. 20.

Soheil Eshghi (S'09–M'10) received the B.Sc. degree in electrical engineering from Sharif University of Technology, Tehran, Iran, in 2010, and the M.S.c. degree in electrical engineering from the University of Pennsylvania, Philadelphia, PA, USA, in 2013, and is currently pursuing the Ph.D. degree in electrical and systems engineering at the University of Pennsylvania.

His research interests are in optimal control, stochastic optimization, network epidemiology, and optimal operation of smart grids.

M. H. R. Khouzani received the B.Sc. degree in electrical engineering from Sharif University of Technology, Tehran, Iran, in 2006, and the M.S.E. and Ph.D. degrees in electrical and systems engineering from the University of Pennsylvania (UPenn), Philadelphia, PA, USA, in 2008 and 2011, respectively, with a fellowship award under the supervision of Prof. Saswati Sarkar.

Since 2011, he has held postdoctoral research appointments with The Ohio State University, Columbus, OH, USA, and the University of Southern California, Los Angeles, CA, USA. Currently, he is with the Information Security Group (ISG), Royal Holloway University of London, Egham, U.K. His research interests are in applications of optimization, optimal control, and game theory in cyber-security and communication networks.

Dr. Khouzani's Ph.D. thesis received the 2012 Joseph and Rosaline Wolf Award of best dissertation among male students in Electrical and Systems Engineering at UPenn.

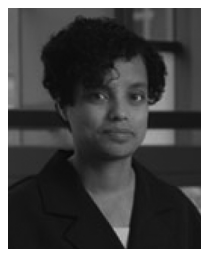

Saswati Sarkar (S'97–M'01) received the M.E. degree in electrical communication engineering from the Indian Institute of Science, Bangalore, India, in 1996, and the Ph.D. degree in electrical and computer engineering from the University of Maryland, College Park, MD, USA, in 2000.

She joined the Electrical and Systems Engineering Department, University of Pennsylvania, Philadelphia, PA, USA, as an Assistant Professor in 2000, and is currently a Professor. Her research interests are in stochastic control, resource allocation, dynamic games, and economics of networks.

Prof. Sarkar was an Associate Editor of the IEEE TRANSACTIONS ON WIRELESS COMMUNICATIONS from 2001 to 2006, and of the IEEE/ACM TRANSACTIONS ON NETWORKING from 2008 to 2013. She received the Motorola gold medal for the best master's student in the division of electrical sciences at the Indian Institute of Science and a National Science Foundation (NSF) Faculty Early Career Development Award in 2003.

Santosh S. Venkatesh (S'81–M'86–SM'14) received the Ph.D. degree in electrical engineering from the California Institute of Technology, Pasadena, CA, USA, in 1986.

He is a Professor with the Department of Electrical and Systems Engineering, University of Pennsylvania, Philadelphia, PA, USA. His research interests are in probabilistic models, random graphs, epidemiology, and network and information theory.